LBL-24211 c.2
UC-400

Lawrence Berkeley Laboratory
UNIVERSITY OF CALIFORNIA

APPLIED SCIENCE DIVISION

FY 1987 Annual Report

RECEIVED
LAWRENCE
BERKELEY LABORATORY

AUG 31 1988

LIBRARY AND
DOCUMENTS SECTION

Energy Conversion and Storage Program

March 1988

TWO-WEEK LOAN COPY
This is a Library Circulating Copy
which may be borrowed for two weeks.

APPLIED SCIENCE
DIVISION

LBL-24211 c.2

Prepared for the U.S. Department of Energy under Contract Number DE-AC03-76SF00098.

DISCLAIMER

This document was prepared as an account of work sponsored by the United States Government. While this document is believed to contain correct information, neither the United States Government nor any agency thereof, nor the Regents of the University of California, nor any of their employees, makes any warranty, express or implied, or assumes any legal responsibility for the accuracy, completeness, or usefulness of any information, apparatus, product, or process disclosed, or represents that its use would not infringe privately owned rights. Reference herein to any specific commercial product, process, or service by its trade name, trademark, manufacturer, or otherwise, does not necessarily constitute or imply its endorsement, recommendation, or favoring by the United States Government or any agency thereof, or the Regents of the University of California. The views and opinions of authors expressed herein do not necessarily state or reflect those of the United States Government or any agency thereof or the Regents of the University of California.

LBL-24211

APPLIED SCIENCE DIVISION ANNUAL REPORT

ENERGY CONVERSION AND STORAGE PROGRAM

FY 1987

Elton J. Cairns
Program Leader
Head, Applied Science Division
and
Associate Director, LBL

Applied Science Division
Lawrence Berkeley Laboratory
University of California
Berkeley, California 94720

Prepared for the U.S. Department of Energy under Contract No. DE-AC03-76SF00098

CONTENTS

Introduction 1-1

ELECTROCHEMICAL ENERGY STORAGE AND CONVERSION

Technology Base Research Project for Electrochemical Energy Storage
E.J. Cairns, K. Kinoshita, and F.R. McLarnon 1-2

Advanced Electrode Research
E.J. Cairns, F.R. McLarnon, T.C. Adler, M.J. Isaacson, K.G. Miller, S.A. Naftel, J. Rudnicki, and K.A. Striebel 1-4

THERMAL ENERGY STORAGE AND CONVERSION

Direct Solar Thermal Conversion Processes
A. Hunt, I. Hodara, F. Miller, and J. Noring 1-12

Microstructured Materials
A. Hunt, F. Hibbler, P. Hsuin, and K. Lofftus 1-14

Light Scattering Studies
A. Hunt, C. Gross, K. Lofftus, A. Quintanilha, M. Quinby-Hunt, F. Livolat, and M. Maestre 1-15

Solid-State Radiative Heat Pump
P. Berdahl 1-17

COAL-RELATED RESEARCH

Processing of Condensate Waters from Coal Gasification
C.J. King, J. Senetar, T. Grant, L. Poole, and R. Thompson 1-19

Removal of H_2S from Coal-Derived Gases
S. Lynn, R. Hix, D. Neumann, S. Sciamanna, and C. Stevens 1-20

Analysis of Coal Gasification Reactors
M.M. Denn and G. Dow 1-23

ENERGY-RELATED CHEMISTRY

Energy-Related Organometallic Chemistry
R.H. Fish, J.G. Reynolds, R.H. Fong, A.D. Thormodsen, R.B. Beser, Jr., H-S. Kim, G. Friedman, and R.T. Price 1-25

Ammonia Removal from Oil Shale Process Waters Using Tubular, Microporous Polytetrafluoroethene Membranes
R.H. Sakaji, C.G. Daughton, R.E. Selleck, and J.F. Thomas 1-29

Kinetics of Gas-Phase Reactions Between Ozone and Selected Nitrogen Heterocycles from Oil Shale Wastes
E.R. Blatchley III, J.F. Thomas, and C.G. Daughton 1-32

Separations by Reversible Chemical Association
C.J. King, A.S. Kertes, D. Arenson, J. Tamada, W. Rixey, A. Garcia, L. Poole, and M. Ng 1-34

Differential Photothermal Deflection Spectroscopy
R.E. Russo, J.D. Spear, and R.J. Silva 1-36

ENERGY CONVERSION AND STORAGE PROGRAM STAFF

Elton Cairns, Program Leader
Harvey Blanch, Deputy Program Leader
Michael Wahlig, Deputy Program Leader

Thomas Adler
Daniel Arenson
Vincent Battaglia
Paul Berdahl
Ernest Blatchley
Garth Burns
Van Carey
Douglas Clark
Thomas Colson
Daniel Crean
Ayesha Daniels
Christian Daughton
Morton Denn
Gregory Dow
Katherine Dukes
Jean Dupon
Richard Fish
Raymond Fong
Alan Foss
Gad Friedman*
Antonio Garcia
Terry Grant
Edward Grens
Robert Guinn
Donald Hanson
Richard Hix
Isaac Hodara*
Paul Hsuin
Arlon Hunt
Mark Isaacson
Alejandro Izquierdo
Avieyer Kertes
Hoon-Sik Kim
C. Judson King
Kim Kinoshita
Judith Klinman
Gregg Langlois
Susan Lauer
Laura Lindsay-Murphy
Kevin Lofftus
Scott Lynn
Frank McLarnon
Fletcher Miller
Kenneth Miller
Riley Moore
Stuart Naftel
Mindy Ng
Dan Neumann
Jon Noring
Loree Poole
Robert Price
William Rixey
James Rudnicki
Richard Russo
Richard Sakaji
Steve Sciamanna
Robert Selleck
Jon Spear
Charlotte Standish
John Starr
Craig Stevens
Kathryn Striebel
Janet Tamada
Jerome Thomas
Jeffrey Weaver
Charles Wilke

*Participating Guest.

ENERGY CONVERSION AND STORAGE

INTRODUCTION

The Energy Conversion and Storage Program has four main projects applying chemistry and chemical engineering to problems in the production of new fuels, their environmental impact, and energy storage and conversion. These projects are:

(1) Electrochemical energy storage and conversion
(2) Thermal energy storage and conversion
(3) Coal-related research
(4) Energy-related chemistry

Each of these projects focuses on transport-process principles, chemical kinetics, thermodynamics, separation processes, and organic and physical chemistry, and advanced analysis methods.

The electrochemical energy storage and conversion project provides research to develop advanced power systems for electric vehicle and stationary energy storage applications. Topics include identification of new electrochemical couples for advanced rechargeable batteries, improvements in battery and fuel cell materials, and the establishment of engineering principles applicable to electrochemical energy storage and conversion. Major emphasis is on applied research that will lead to superior performance and lower life-cycle costs.

The second project is a series of research and development efforts in thermal energy storage and conversion. This project focuses on new and innovative approaches to the more efficient utilization of thermal and solar energy.

The third project involves the development of improved, energy-efficient methods for processing waste streams from synfuel plants and coal gasifiers. Also included in this project is an effort to develop an advanced model of moving-bed coal gasifiers in order to better understand their operation and improve their design.

The last project addresses the identification, characterization, and separation of components in liquid fuel system streams. On-going research topics include the use of advanced methods to remove nitrogen-containing compounds from petroleum feedstocks and wastestreams, the synthesis and characterization of complex organometallic compounds, the development of innovative methods to remove trace heavy metal compounds from fossil materials, and the study of biomimetic reactions to carry out the hydroxylation of hydrocarbons. Novel processes, such as separations by reversible chemical association, are being developed to recover valuable organic products from dilute aqueous solutions that result from the fermentation of biomass. In addition, ultra-sensitive spectroscopic techniques are being applied to detect trace amounts of materials.

ELECTROCHEMICAL ENERGY STORAGE AND CONVERSION

Technology Base Research Project for Electrochemical Energy Storage*

E.J. Cairns, K. Kinoshita, and F.R. McLarnon

The Lawrence Berkeley Laboratory (LBL) is lead center for management of the Technology Base Research (TBR) Project, which is supported by the Electrochemical Branch of DOE's Office of Energy Storage and Distribution. The purpose of this project is to provide the research base to support DOE efforts to develop electrochemical energy conversion systems for electric vehicle and stationary energy storage applications. The specific goal is to identify the most promising electrochemical technologies and transfer them to industry and/or another DOE program for further development and scale-up.

The general research areas addressed by the TBR Project include identification of new electrochemical couples for advanced batteries, determination of technical feasibility of the new couples, improvements in battery components and materials, establishment of engineering principles applicable to electrochemical energy storage and conversion, and the investigation of fuel cell and metal/air systems for transportation applications. Major emphasis of the project is given to applied research that will lead to superior performance and lower life-cycle costs.

The LBL scientists who participate in the project are E.J. Cairns, K. Kinoshita and F.R. McLarnon of the Applied Science Division, and L.C. DeJonghe, J.W. Evans, R.H. Muller, J.S. Newman, P.N. Ross and C.W. Tobias of the Materials and Chemical Sciences Division.

ACCOMPLISHMENTS DURING FY 1987

LBL conducted a vigorous in-house research program and monitored 25 subcontracts during FY 1987. A description of the research projects conducted by the subcontractors can be found in the recent annual report, *Technology Base Research Project for Electrochemical Energy Storage* (LBL-23495), and the in-house work, "Electrochemical Energy Storage," is summarized in the next article and in the *Materials and Chemical Sciences Division 1987 Annual Report* (LBL-24242). Highlights of the subcontracted work follow:

Exploratory Research

- Efforts continue at Argonne National Laboratory (ANL) on testing of 20-Ah $LiAl/FeS_2$ cells containing a dense upper-plateau FeS_2 electrode, a Li-Al electrode, and LiCl-LiBr-KBr electrolyte (m.p. 310°C). The cycle-life stability of cells containing 15-mol% CoS_2 in the positive electrode is being evaluated in an accelerated test. A cell has been operating for over 300 deep discharge cycles with a capacity loss of about 4%. Experiments are now underway to demonstrate overcharge protection of lithium-limited cells.
- Gould, Inc. has focused their efforts on cell design and construction to improve the hermeticity of Li-alloy/FeS_2 cells. A new cell design incorporating a glass-metal feedthrough attached to the cover and an all-welded construction is under evaluation.
- Experimental measurements at the University of Pennsylvania demonstrated that poly(ethylene oxide) [PEO] containing a Mn(II)/Mn(III) redox couple with the composition $(PEO)_nMnBr_2$ (n = 8 or 16) shows interesting properties for use in positive electrodes for ambient-temperature lithium cells.
- The University of Minnesota is investigating the mechanisms of reactions occurring at the electrode/electrolyte interface of novel electrochemical cells containing thin-film polymer electrolytes. Experiments are currently underway on electrodes containing sodium and divalent metals, such as zinc, magnesium and calcium, and PEO electrolyte.
- EIC Laboratories, Inc. has developed a novel low-temperature chemical synthesis method to produce lithium anode materials such as Li-Al, Li_xWO_2, $Li_xFe_2O_3$ and $LiCoO_2$ for rechargeable lithium cells containing organic electrolytes and metal-oxide cathodes.

*This work was supported by the Assistant Secretary for Conservation and Renewable Energy, Office of Energy Storage and Distribution of the U.S. Department of Energy under Contract No. DE-AC03-76SF00098.

Applied Science Research

- Two major areas of focus of the research project at Stanford University are: (i) develop replacements for the negative electrode/β''-Al_2O_3 assembly in the Na/β''-Al_2O_3/$NaAlCl_4$/$FeCl_2$ (Zebra) cell, and (ii) preparation of thin-layer electrode and electrolyte materials by high-rate atmospheric pressure chemical vapor deposition (CVD) techniques. A combination of sodium alloy electrode and $NaAlEt_4$ (Et = ethyl group) liquid electrolyte appears to be an attractive alternative to the Na /β''-Al_2O_3 assembly in Zebra cells. Initial experiments with the CVD apparatus demonstrated that thin films of $FeS_{1.5}$ can be easily produced.
- ANL has encountered some difficulty in preparing glass tubing from a glass with a composition (42 mol% Na_2O - 8 mol% Al_2O_3 - 5 mol% ZrO_2 - 45 mol% SiO_2) that was previously identified as a candidate solid electrolyte for use in high-temperature Na/S cells. An alternative fabrication process has been recently developed that allows the production of glass tubes of sufficient quality and quantity for sealed-cell testing.
- Massachusetts Institute of Technology has identified glasses with adequate lithium-ion conductivity for battery applications, but improved stability in lithium and sulfur environments is required. Preliminary measurements indicate that calcium-containing lithium borate glasses are stable at high lithium activities.
- The Illinois Institute of Technology (IIT) has successfully electrodeposited Mo and Mo_2C layers from a FLINAK (LiF-NaF-KF) melt. The corrosion rates of these materials in Na_2S_3 melts at 300°C indicates they may be suitable for use as coatings on containment materials in Na/S cells.
- Brookhaven National Laboratory (BNL) has continued EXAFS (Extended X-ray Absorption Fine Structure) studies of zinc bromide electrolytes. Analysis of a dilute electrolyte (0.1 M $ZnBr_2$) indicates that the bromide ions are surrounded by a very loosely bound hydration sheath with a Br-O distance of ~3.0Å. At higher concentration (3 M $ZnBr_2$) only two waters of hydration are associated with the bromide ions.
- The effects of transport processes on the kinetics and morphology of zinc deposition in acidic electrolytes are being investigated by IIT. The propagation of zinc dendrites can be almost completely suppressed at a rotating cylinder electrode (at 400 rpm rotation speed) up to a loading of ~140 mAh/cm^2.
- Surface science methods (thermal desorption, low-energy electron diffraction, work function, Raman) are being applied at Case Western Reserve University (CWRU) and Jackson State University to characterize the surface of reactive alkali and alkaline earth metals in organic electrolytes. Raman spectroscopy indicates that Li_2CO_3 and Li_2O are formed on a lithium surface in propylene carbonate (PC).
- Johns Hopkins University is investigating the corrosion resistance of commercial materials in organic electrolytes. Their studies show that the presence of water in organic electrolyte (0.5 M $LiClO_4$/PC) has a strong influence on the corrosion of Armco steel. As the water content in PC decreases, Armco steel becomes more susceptible to localized attack because it cannot be readily passivated.

Air Systems Research

- Efforts continue at CWRU to develop more effective electrocatalysts for oxygen reduction and generation. The studies indicate that transition metal oxides are active catalysts for oxygen generation and peroxide decomposition, but they have shown poor activity for oxygen reduction in alkaline electrolytes. However, heat treatment of a mixture of a transition metal organic macrocycle (cobalt octaethylporphyrin supported on Vulcan XC-72) and $La_{0.8}Sr_{0.2}Co_{0.9}Ru_{0.1}O_3$ perovskite has shown good activity for oxygen reduction in 4 M NaOH at 60°C.
- Experiments at Pinnacle Research Institute demonstrated that further improvement in the discharge performance of zinc/air cells with flowing electrolyte is possible with the use of a combination of additives. The addition of 25 g/l silicate (SiO_2) + 15 g/l sorbitol to 12 M KOH increased the zinc capacity from 87.2 Ah/l to 191.3 Ah/l and the zinc utilization (300 g/l initially at full charge) from 35.45 to 77.79% at a discharge current density of 200 mA/cm^2.
- Experiments are underway at SRI International to investigate the rate and mechanism of aluminum corrosion in KOH electrolyte in Al/air batteries. Aluminum alloys containing Li and In were found to exhibit quite negative potentials (to -1.755 V versus Hg/HgO) but also displayed high corrosion rates (260-340

mA/cm^2). Alloys containing In, Mg and Mn also exhibited negative potentials (-1.790 to -1.820 V), but showed somewhat lower corrosion rates (75 to 118 mA/cm^2).

- Los Alamos National Laboratory (LANL) has improved the fabrication process for air electrodes in proton-exchange membrane (PEM) fuel cells. By optimizing the hot pressing conditions used to fabricate the Prototech electrode and Nafion membrane structure, and increasing the surface concentration of Pt by sputtering a thin film of Pt onto the structure, a significant improvement in performance at current densities to 1 A/cm^2 was observed. These results demonstrate that mass-transport limitations in PEM fuel cells can be greatly reduced.
- EXAFS was utilized by BNL to characterize heat-treated macrocycles (cobalt and iron tetramethoxyphenyl porphyrins (TMPP)) for O_2 reduction in fuel cells. For Fe-TMPP supported on Vulcan XC-72, EXAFS revealed that a FeN_4 structure remained after heat treatment at 900 and 1000°C. This type of moiety was reported in independent studies by CWRU to be active for O_2 reduction.

PROGRAM CHANGES IN 1987

Funding support for the following project was initiated in 1987:

- Development of Anode Alloys for Aluminum/Air Batteries – SRI International.

The following work was completed in 1987:

- Ambient-Temperature Secondary Lithium Batteries Using LiAl or Lithium Insertion Anodes – EIC Laboratories, Inc.
- Transport in Aqueous Battery Systems – Lawrence Livermore National Laboratory.
- Aluminum/Air Power Cell Research and Development – Lawrence Livermore National Laboratory.

PLANNED ACTIVITIES FOR FY 1988

New initiatives include the following:

- Zinc/Air Battery R&D.
- *In Situ* Studies of Electrode Surfaces.

Advanced Electrode Research*†

E.J. Cairns, F.R. McLarnon, T.C. Adler, M.J. Isaacson, K.G. Miller, S.A. Naftel, J. Rudnicki, and K.A. Striebel

The purpose of this research is to study the behavior of electrodes used in secondary batteries and fuel cells, and to investigate practical means for improving their performance and lifetime. Systems of current interest include ambient-temperature rechargeable cells with Zn electrodes (Zn/air, Zn/NiOOH, Zn/AgO, Zn/Cl_2, Zn/Br_2, and Zn/$Fe(CN)_6^{-3}$); rechargeable high-temperature cells (Li/S, Li-Al/FeS_2, Li-Si/FeS_2, and Na/S); fuel cells; and liquid-junction photovoltaic cells. The approach used in this investigation is to study life- and performance-limiting phenomena under realistic cell operating conditions.

ACCOMPLISHMENTS DURING FY 1987

ALKALINE ZINC ELECTRODES

Rechargeable alkaline Zn/air and Zn/NiOOH cells can be designed to deliver high specific energy and specific power, but they typically exhibit short lifetimes. The high solubility of Zn species in alkaline electrolytes tends to enhance the various physiochemical processes (active material redistribution, filamentary Zn growths, etc.) which degrade the cell's capacity and limit its life. Modeling and experimental investigations are aimed at understanding the

*This work was supported by the Assistant Secretary for Conservation and Renewable Energy, Office of Energy Storage and Distribution of the U.S. Department of Energy under Contract No. DE-AC03-76SF00098.

†This project is part of a larger effort, "Electrochemical Energy Storage," described in the Materials and Chemical Sciences Division 1987 Annual Report (LBL-24242).

complex transport processes in operating Zn electrodes, and characterizing various methods to reduce Zn species solubility and extend the lifetime of the Zn electrode.

Measurement of Concentrations in Porous Zinc Electrodes Using Micro-Electrodes

(M.J. Isaacson, E.J. Cairns and F.R. McLarnon)

Zn and Cd μ-electrodes have been used to investigate processes in cycling porous Zn electrodes.[1] Electrodes were cycled for 30 to 60 cycles in the 17% and 30% KOH. The active material tended to redistribute towards the center of the electrode in cells with 17% KOH electrolyte, and toward the edges of the electrode in 30% KOH electrolyte, as was previously observed in this laboratory.[2]

During the first 20 to 30 cycles the Zn and the Cd μ-electrode potentials changed very little as the electrode was charged and discharged. The potential differences between the μ-electrodes were usually only about 2-4 mV at any particular time, although they changed by about 10-20 mV during a cycle. Surprisingly, a potential minimum was frequently observed near the beginning of a charge. Small potential gradients were observed at the edge of the electrode in the 17% cell, which correlated well with the position of the edge of the electrode. It was not apparent whether the potential gradients were due to secondary current distribution or to a decrease in the porosity near the electrode edge as material moved toward the center of the electrode.

As cycling continued "structure" started to develop in the Zn μ-electrode data, as seen in Fig. 1. The Cd μ-electrodes also showed an increase in polarization but to a much smaller extent, and later during the cycling than the Zn μ-electrodes. Calculated molalities showed that the increase in μ-electrode polarization was almost entirely due to changes in the $Zn(OH)_4^{2-}$ concentration, which often decreased to 10% of the nominal concentration during charge and increased to 300% of the nominal concentration during discharge. X-ray photographs of the electrodes indicated that the largest changes in the μ-electrode potentials and concentrations occurred in areas which may have experienced an increase in current density due to material redistribution.

The μ-electrode potentials and molalities indicate that the electrode is not limited by transport of reactants and products in early cycles. However as cycling continues and material redistribution occurs the electrode becomes limited by transport of

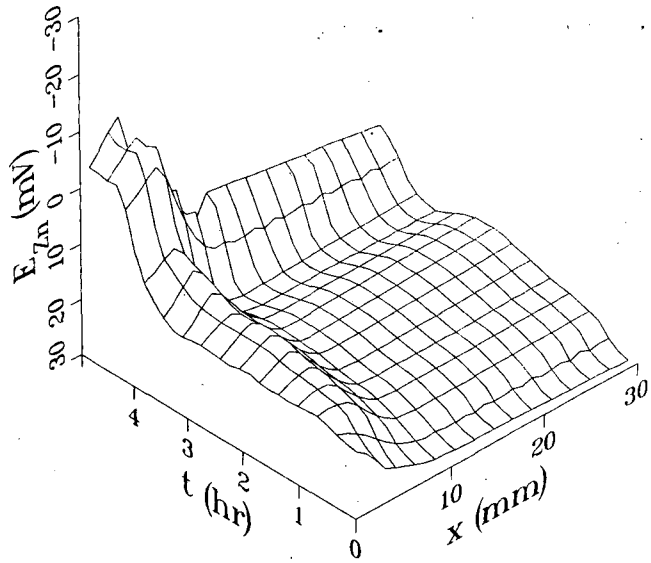

Figure 1. Zn μ-electrode potentials during charge cycle 32 in 30% KOH electrolyte. (XBL 882-577)

$Zn(OH)_4^{2-}$, dissolution of ZnO, or precipitation of $Zn(OH)_4^{2-}$. This limitation is probably due to an increase in the current density and a decrease in the electrode porosity in areas where the μ-electrode polarization is increasing.

Mathematical Modeling of the Zinc Electrode

(K.G. Miller, E.J. Cairns and F.R. McLarnon)

The one-dimensional, time-dependent model reported earlier[3] has now been implemented.[4] This model is designed to elucidate the the cause of active material redistribution in the Zn electrode, and it takes into account transport of electrolyte species, heterogeneous reactions, kinetics, and current density variations.

A simplified version of this model, where the concentration terms are omitted from the equations for Ohm's Law in the electrolyte phase and the electrolyte velocity is assumed to be zero, provides insight into the transient electrolyte changes over the course of one cycle. The results for the changes in the concentrations of zincate ion ($Zn(OH)_4^{2-}$) and hydroxide ion (OH^-) are shown for both Zn and Ni electrode compartments for one cycle (5.0 hour charge, 15 minute open-circuit, 2.5 hour discharge) in Fig. 2. The concentrations represent a particular location in the center of the cell. The results were found to be very sensitive to the value of the precipitation/dissolution rate constants, and the values used in the results presented here were both

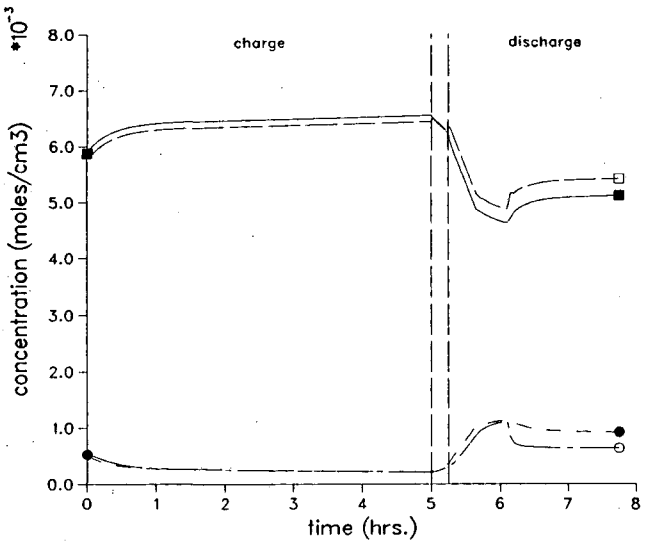

Figure 2. Calculated concentrations from Zn/NiOOH cell model for one cycle (5.0-hour charge, 15-minute open-circuit, 2.5-hour discharge). The precipitation/dissolution rate is 2.5×10^{-5} cm/sec. These concentrations are at a particular location in the middle of the cell. Symbols represents concentrations as follows: ■, OH^- in the Zn compartment; □, OH^- in the Ni compartment; ●, $Zn(OH)_4^{2-}$ in the Zn compartment; ○, $Zn(OH)_4^{2-}$ in the Ni compartment. (XBL 882-578)

2.5×10^{-5} cm/sec. Another important point concerns the onset of precipitation or dissolution of ZnO. Experimentally, it has been found that when a KOH solution is undersaturated with $Zn(OH)_4^{2-}$, ZnO will always dissolve. However, during discharge, it has been found the electrolyte can supersaturate to about three times the equilibrium concentration of $Zn(OH)_4^{2-}$. Therefore, the model was developed so that whenever the electrolyte was undersaturated, dissolution of ZnO always occurred. When the electrolyte became supersaturated in $Zn(OH)_4^{2-}$, precipitation was not allowed to occur until the concentration of $Zn(OH)_4^{2-}$ was three times its saturation value. The following trends have been found from the model:

(1) By the end of the charge cycle, the concentration of OH^- increases only about 15% whereas the concentration of $Zn(OH)_4^{2-}$ decreases by about a factor of 50% from their initial values.

(2) The differences in concentrations of both $Zn(OH)_4^{2-}$ and OH^- in the Zn and NiOOH electrode compartments are not very large during charge. This shows there is good movement from one side of the microporous separator to the other.

(3) During discharge, the concentrations of both $Zn(OH)_4^{2-}$ and OH^- change much more than during the charge cycle. This is due to supersaturation of the electrolyte with $Zn(OH)_4^{2-}$. After precipitation of zincate (as ZnO) occurs the concentrations remain relatively unchanged. Also, the concentration differences between the Zn and Ni electrode compartments are much greater after precipitation starts, during discharge. This could be explained by the fact that the precipitation of zincate (as ZnO) was observed to be faster in the Zn compartment due to the higher concentration of $Zn(OH)_4^{2-}$ in the Zn compartment than in the Ni compartment.

In addition, the model was run at different rates of precipitation/dissolution to see what effect this parameter had on the results. During charge, if the value was set at 5.0×10^{-5} cm/sec, there was very little change in the concentrations of both $Zn(OH)_4^{2-}$ and OH^- from their initial values. However, if the rate was set at 1.5×10^{-5} cm/sec, the concentration of $Zn(OH)_4^{2-}$ dropped nearly to zero by the end of charge. This demonstrates that there is only a narrow value of this parameter that gives meaningful results.

Investigations of Methods to Improve Zinc/Nickel Oxide Cell Lifetime

(T.C. Adler, F.R. McLarnon, and E.J. Cairns)

Three factors under investigation for improving Zn/NiOOH cell cycle-life performance are: 1) electrolyte composition,[2] 2) electrode composition,[5] and 3) charging method.[6] Zn/NiOOH cells using 25-33 mol% $Ca(OH)_2$-additive in the Zn electrodes, 31 wt% KOH or 15 wt% KOH-15 wt% KF electrolytes, and a 30-ms on/90-ms off pulse-charging regimen were investigated.[7] Although one of these cells lasted for over 500 cycles, they generally failed from dendritic shorting within 20-60 cycles. The $Ca(OH)_2$-additive electrodes cycled in 31 wt% KOH exhibited diamond-shaped crystals characteristic of $CaZn(OH)_4$. No such crystals were observed in $Ca(OH)_2$ additive electrodes cycled in KOH-KF electrolyte because CaF_2 is thermodynamically favored over $CaZn(OH)_4$. An electrode of pure $CaZn(OH)_4$ cycled at constant current in 31 wt% KOH was well-behaved and showed a very uniform distribution of material after 50 cycles, much better than observed with the $Ca(OH)_2$-additive electrodes. Cells containing negative electrodes of ZnS and ZnSe, having very low solubilities in 31 wt% KOH, produced very high

overpotentials on formation, along with low charging efficiencies. Several new separator materials were evaluated, but none of them provided a superior barrier to dendrite penetration, as compared to three layers of microporous polypropylene (Celgard).

The cells described above transferred Zn to the NiOOH electrode at the same rate as standard Zn-electrode cells. An average of 45% of the weight gained by the Ni electrode during cycling was present as Zn, consistent with the interpretation that Zn ions displaced Ni ions in the α-nickel hydroxide hydrate of the Ni electrode. Impregnating the NiOOH electrode with ZnO prior to cycling might slow the rapid transfer of Zn to the NiOOH electrode in the early cycling of the cell, and allow the Zn electrode to be reduced in weight, maintaining satisfactory specific energy. Mechanical deposition of ZnO from an aqueous slurry into the NiOOH electrode on a vacuum table loaded only about one-fourth the amount required, so this may need to be carried out by an electrochemical process.

The computer-controlled cell cycling system is being modified for charging cells in a constant-voltage, limited-current mode which prevents the occurrence of high overpotentials associated with the formation of Zn dendrites.

HIGH-TEMPERATURE CELLS

The high-temperature Na/S cell offers very good performance, and recent improvements to the process for manufacturing the ceramic β''-Al_2O_3 electrolytes indicate that acceptable cell lifetimes may be realized. However, the performance of the sulfur electrode has not been optimized, and the phenomena which govern its operation are poorly understood. On-going work is aimed at developing and confirming an advanced mathematical model of the sulfur electrode.

Mathematical Modeling of the Sodium/Sulfur Cell

(S.A. Naftel, F.R. McLarnon and E.J. Cairns)

A comprehensive model of the sulfur electrode in Na/S cells has been developed.[8,9] The cell being modeled is of the tubular central-sodium type, and includes a thin layer of α-alumina felt around the β''-alumina solid electrolyte,[10,11] in order to prevent deposition of sulfur on the solid electrolyte during cell charge. The model consists of a set of non-linear PDE's which describes the processes of diffusion, migration, and convection which take place during the operation of such a cell. Solution of the linearized equations is effected on a digital computer via implementation of the Newman-IAD method,[12] a finite-difference technique for the solution of second order linear PDE's.

Fluid flow through the sulfur electrode, which is essentially a porous graphite felt, is accounted for by use of the differential form of Darcy's law, $\mathbf{v} = k\nabla P$, for flow through porous media. This requires the use of capillary pressure and relative permeability, both of which are functions of the fluid-matrix system.[13] Due to the difficulty of performing measurements on the sulfur/polysulfide/graphite system directly, an analogous system (water/bromobenzene/glass fiber) was used. Theory[14] was then applied in order to estimate the capillary pressure and relative permeability values for the system of interest, using the experimental data. Figure 3 shows the relative permeability of the sulfur (wetting) and polysulfide (non-wetting) phases as functions of the saturation (volume fraction). Beyond a value of saturation of 0.75, the polysulfide phase is no longer interconnected, and it does not

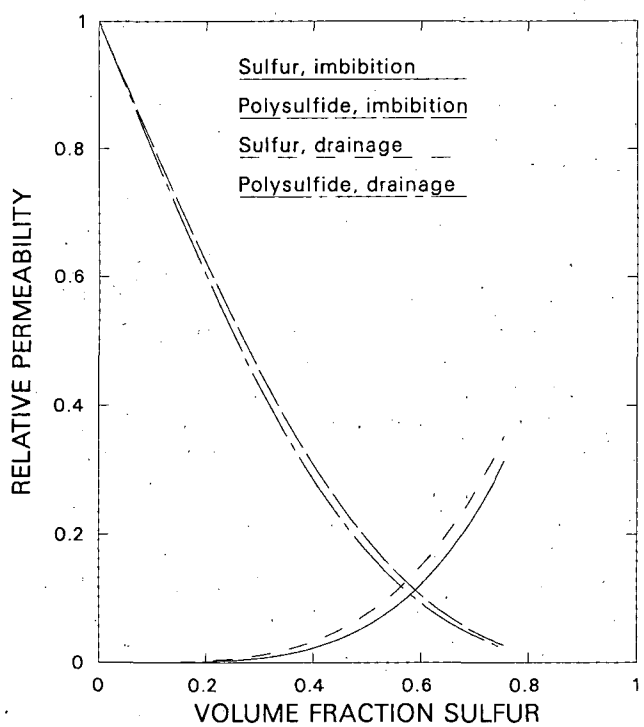

Figure 3. Computed values of relative permeability of sulfur and sodium polysulfide in graphite felt. Values are shown for both the imbibition(displacement of polysulfide by sulfur), and the drainage(replacement of sulfur by polysulfide) cycles. Beyond a sulfur volume fraction of 0.78, the polysulfide phase is discontinuous and no longer moves. (XBL 882-579)

move. The relative permeabilities of the sulfur and polysulfide phases are 1 and 0 respectively in this region. The only other physical property remaining to be measured is the graphite felt conductivity. All other physical properties are available in the literature.

The results of this modeling will be compared with data from an operating cell which has been designed to allow measurement of ionic potentials throughout the sulfur electrode. An attempt will be made to predict the effect of various charge-discharge regimens upon cell operation.

FUEL CELLS

Fuel cells can be designed to exhibit acceptable lifetimes for a number of applications. However, the performance of the O_2 electrode in fuel cells requires improvement, and the development of an efficient direct-methanol fuel cell would represent a major advance over reformed-hydrocarbon fuel cells.

Application of PDS to Electrochemical Interfaces

(J. Rudnicki, E.J. Cairns and F.R. McLarnon)

Photothermal deflection spectroscopy (PDS) has been developed as a sensitive *in-situ* method for investigation of electrochemical interfaces.[15-17] This method is a novel application of PDS, and should prove to be an exceptional addition to the few *in-situ* techniques currently in use. An advantage of this technique is that the electrode surface is not required to be optically smooth. The same system is also used to simultaneously measure concentration gradients adjacent to the electrode surface. This additional information is helpful in determining the surface chemistry. Various types of electrochemical interfaces can be studied by this method, e.g., corrosion, secondary electrodes, and electrocatalysts. The objective of this work is to study direct electro-oxidation of methanol on Pt ad-atom catalysts. Increased understanding of these catalysts will aid in the development of high-performance direct methanol-air fuel cell systems.

PDS is a comparatively simple system. Monochromatic light is directed through the electrolyte and onto the electrode at a normal incidence. Absorption of light by the surface causes heating of the electrode and thereby forms a thermal gradient adjacent to the electrode. Index of refraction is a function of temperature; an associated gradient in the index of refraction is formed. A probe laser beam is directed parallel to the electrode through this gradient and is deflected. The magnitude of this deflection is proportional to the surface absorption. Modulation of the light source and lock-in detection are implemented to increase the signal-to-noise ratio.

Electrochemical reactions will create concentration and associated refractive-index gradients, which can be measured by the probe beam. Since this deflection is not modulated, it can be discriminated from the deflection due to the surface absorption by the lock-in instrumentation, yielding simultaneous measurement of surface absorption and concentration gradients.

The primary parameter measured by PDS is the absorption of light at a surface. Scanning of the wavelength of the source allows spectra of the interfacial species to be obtained. Confirmation experiments on systems with known spectra have been successful. Absorption can be measured at constant wavelength while the electrode potential is changed. Cyclic voltammetry of Pt in 0.1 M $HClO_4$ along with the corresponding absorption and concentration gradient is shown in Fig. 4. This experiment shows that PDS is sensitive to the formation of single layers of molecules at the surface; in this case, the formation of platinum oxide is clearly seen. The microscopic concentration gradients formed are also evident.

Preliminary experiments on the oxidation of methanol on Pt and an under-potential deposition (UPD) process by which ad-atom catalysts are formed have shown that PDS will be an effective tool to increase the understanding of these systems. Developmental effort is under way to extend the spectral range of the system into the infra-red. This would allow *in-situ* vibrational spectra to be obtained, which can help identify organic surface species.

Oxygen Reduction In Alkaline Fuel Cell Electrolytes

(K.A. Striebel, E.J. Cairns and F.R. McLarnon)

Voltage losses in the O_2 cathode represent the major inefficiency in aqueous fuel cells for transportation or stationary applications. Experimental and theoretical studies of oxygen reduction (OR) in aqueous alkaline electrolytes on smooth and supported Pt have been carried out.[18,19]

The mechanism for OR on Pt in alkaline electrolytes is complicated by the concurrent oxidation and reduction of Pt. Rotating ring-disk electrode (RRDE) studies carried out with anodic and cathodic potential sweeps in 0.1 to 6.9 M KOH and 0.1 to 4.0 M

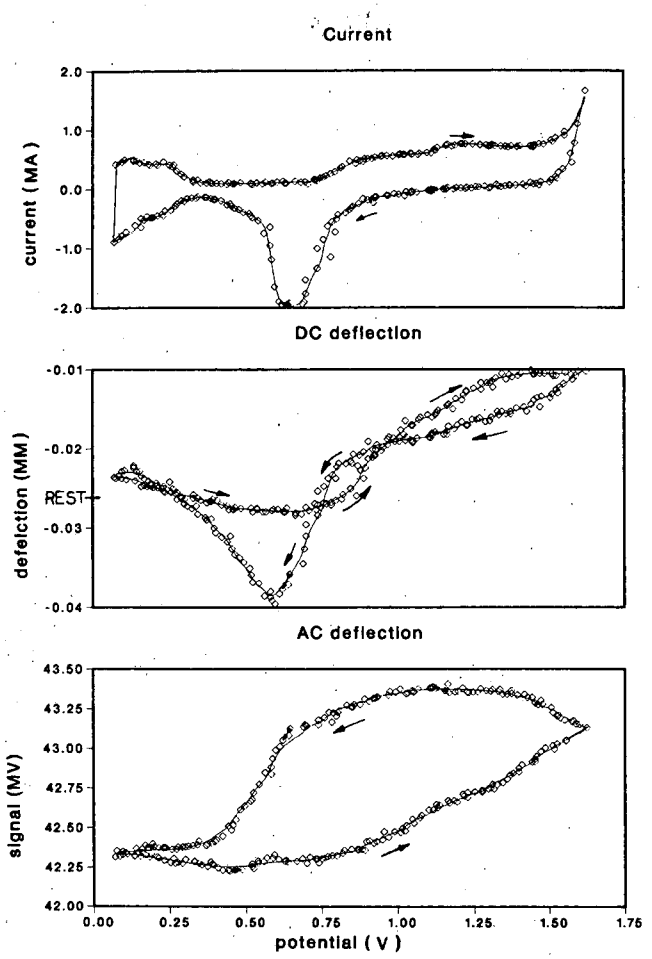

Figure 4. Simultaneous cyclic voltammetry and PDS of Pt in 0.1 M $HClO_4$. The upper plot shows the electrode current response to a cyclic potential scan at 100 mV/s. The DC deflection lot represents the concentration gradients formed in the electrolyte. Deflections positive to the REST deflection indicate that the electrolyte concentration near the electrode is higher than in the bulk, and deflections negative to the REST deflection indicate lower electrolyte concentrations. The AC deflection plot indicates the amount of light absorption at the electrode surface. The excitation light wavelength was 550 nm. (XBL 882-580)

K_2CO_3 revealed similar currents when corrected for O_2 solubility differences. In dilute electrolytes, OR proceeds primarily through the 4-electron pathway to water, independent of pH. In KOH, the mechanism for Pt oxidation changes and the fraction of current yielding a peroxide product increases at 2 to 3 M. These changes were not observed in K_2CO_3.

Porous gas diffusion electrodes (GDE) with supported Pt catalyst were studied in a special cell with low uncompensated solution resistance. Cyclic voltammograms yielded measurements of the wetted areas of carbon and Pt and the local electrolyte composition. GDE galvanostatic steady-state performance with 100% O_2 was measured in 2 to 11 M KOH and 2 to 5.5 M K_2CO_3. Comparisons with kinetic results suggest that OR on carbon contributes to the high currents in 6.9 M KOH at high overpotentials. In K_2CO_3, lower wetted areas and slow OH^- ion transport are responsible for the poor performance when compared with KOH.

Models for the steady-state operation of porous GDE's were developed. These models account for the diffusion and reaction of O_2 and ionic transport in KOH and K_2CO_3. Performance data showed good agreement with the model, using reasonable values for the electrode structural parameters. The non-kinetic Tafel slope and the half-order dependence on O_2 pressure, observed with K_2CO_3, were predicted without using adjustable parameters. Comparison between the model and experiment is shown in Fig. 5. The results suggest that modifications of the GDE structure will be necessary to obtain good performance with aqueous carbonate electrolytes.

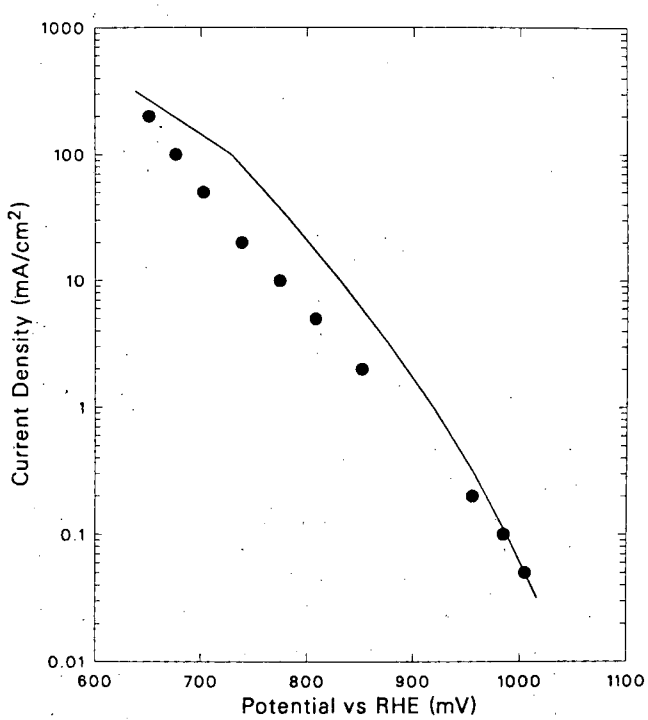

Figure 5. Steady-state model fit to oxygen cathode data recorded in 2M K_2CO_3 electrolyte at 25°C with 1 atm. O_2. (XBL-8711-4714)

PLANNED ACTIVITIES FOR FY 1988

Continuing research efforts on secondary alkaline Zn electrodes will include the cycle-life testing of promising electrode/electrolyte formulations in model cells. An improved mathematical model of the Zn electrode will be fully developed, and cycle-life experiments to verify key features of the model, using *in-situ* microelectrode potential measurements to determine electrolyte species concentrations, will be completed. Optical microscopy and new *in-situ* spectroscopic techniques will be applied to identify the transient species formed during secondary Zn-electrode operation.

A time-dependent, two-dimensional mathematical model of the high-temperature sulfur electrode will be fully developed, and Na/S cell tests will be completed to verify important aspects of the model.

Experiments using porous gas-diffusion electrodes to study O_2 reduction in alkaline-carbonate electrolytes will be completed, and new ad-atom electrocatalysts for high-performance fuel-cell systems will be investigated.

REFERENCES

1. Isaacson, M.J., McLarnon, F.R., and Cairns, E.J. (1987), "Potential and Concentration Gradients in Secondary Zinc Electrodes," 172nd Meeting of the Electrochemical Society, Honolulu, HI, Paper No. 147.
2. Nichols, J.T., McLarnon, F.R., and Cairns, E.J. (1984), "Zinc Electrode Cycle-Life Performance in Alkaline Electrolytes having Reduced Zinc Species Solubility," *Chem. Eng. Commun. 37,* 355.
3. Applied Science Division (1987), Annual Report for FY 1986, LBL-22151, pp. 1-6.
4. Miller, K.G., McLarnon, F.R., and Cairns, E.J. (1987), "Mathematical Model of the Secondary Zn/NiOOH Cell," 172nd Meeting of the Electrochemical Society, Honolulu, HI, Paper No. 149.
5. Jain, R., McLarnon, F.R., and Cairns, E.J. (1985), "Evaluation of Calcium Hydroxide Additives in Secondary Zinc Electrodes," 168th Meeting of the Electrochemical Society, Las Vegas, NV, Paper No. 84.
6. Katz, M.H., Adler, T.C., McLarnon, F.R. and Cairns, E.J. (1988), "The Effect of Pulsed Charging on the Cycle-Life Performance of Zinc/Nickel Oxide Cells," *J. Power Sources 22,* 77.
7. Adler, T.C., McLarnon, F.R. and Cairns, E.J. (1987), "Improvements to the Cycle-Life Performance of the Zn/KOH/NiOOH Cell," Proceedings of the 22nd IECEC, published by AIAA, New York, NY, pp. 1097-1111.
8. Naftel, S.A., McLarnon, F.R. and Cairns, E.J. (1986), "Studies of the Sulfur Electrode in Sodium/Sulfur Cells," 170th Meeting of the Electrochemical Society, San Diego, CA, Paper No. 81.
9. Naftel, S.A., McLarnon, F.R. and Cairns, E.J. (1986), "Experimental and Modeling Studies of the Sulfur Electrode in Sodium/Sulfur Cell," 37th Meeting of the International Society of Electrochemistry, Vilnius, USSR, Paper No. 50-7-91.
10. Karas, B. (1985), "Interpretation of Sodium-Sulfur Cell Characteristics Using an Alternating Current Resistance Technique," *J. Electrochem. Soc. 132,* 1261.
11. Karas, B. and King, R.N. (1985) "The Effects of Current Density, Temperature, and Discharge Beyond Na_2S_3 on Sodium-Sulfur Cell Performance and Life," *J. Electrochem. Soc. 132,* 1266.
12. Van Zee, J., Edmund, M.A. and White, R.E. (1980), "Application of Newman's Technique to Coupled, Nonlinear Partial Differential Equations," *Ind. Eng. Chem. Fundamentals 19,* 438.
13. Scheidegger, A.E. (1974), *The Physics of Flow Through Porous Media,* Third edition, University of Toronto Press, Toronto.
14. Brooks, R.H. and Corey, A.T. (1966), "Properties of Porous Media Affecting Fluid Flow," *Proceedings ASCE, Journal of the Irrigation and Drainage Division 2,* 61.
15. Russo, R.E., McLarnon, F.R., Spear, J.D. and Cairns, E.J. (1987), "Probe Beam Deflection for *In-Situ* Measurements of Concentration and Spectroscopic Behavior During Copper Oxidation and Reduction," *J. Electrochem. Soc. 134,* 2783.
16. Russo, R.E., McLarnon, F.R., Spear, J.D. and Cairns, E.J. (1986), "*In-Situ* Study of Electrode Reactions via Photothermal Deflection Spectroscopy," Federation of Analytical Chemistry and Spectroscopy (FACSS) Conference, 13th Annual Meeting, St. Louis, MO, Paper No. 256.
17. Russo, R.E., McLarnon, F.R., Spear, J.D. and Cairns, E.J. (1986), "Observation of Concentration and Thermal Gradients at the Electrode/Electrolyte Interface Using Photothermal Deflection Spectroscopy," 170th Meeting of the Electrochemical Society, San Diego, CA, Paper No. 731.

18. Striebel, K.A., McLarnon, F.R. and Cairns, E.J. (1987), "Platinum Fuel Cell Cathodes with Aqueous Carbonate Electrolytes," 38th Meeting of the International Society of Electrochemistry, Maastricht, The Netherlands, Paper No. 7.20.

19. Striebel, K.A., McLarnon, F.R. and Cairns, E.J. (1985), "The Effect of Carbonate Ions on the Reduction of Oxygen at Platinum Electrodes in Dilute Alkaline Electrolytes," 167th Meeting of the Electrochemical Society, Toronto, Canada, Paper No. 658.

THERMAL ENERGY STORAGE AND CONVERSION

Direct Solar Thermal Conversion Processes*

A. Hunt, I. Hodara, F. Miller, and J. Noring

In this research area we are exploring advanced concepts in the direct conversion of concentrated solar energy to thermal and chemical forms. Of the four research areas, two involve purely solar thermal processes; the others address the solar heating of catalysts to drive useful chemical reactions. The unifying themes to this research are the study of the absorption of concentrated solar energy by small particles or other microstructures, and the conversion of that energy to other forms. This approach may be applied to heat gases to high temperatures for driving turbogenerators and supplying industrial process heat,[1] or to convert solar energy to chemical forms suitable for storage or transport.[2,3] The concept of entrained particle absorbers was first demonstrated in 1982 with the solar test of the Small Particle Heat Exchange Receiver (SPHER). The test showed that air could be heated to high temperatures by absorption of entrained carbon particles that subsequently oxidized to leave a clear gas stream suitable to power a gas turbine. In the past year we continued to explore new concepts and applications in chemical and thermal solar receivers.

ACCOMPLISHMENTS DURING FY 1987

DIRECT RADIANT HEATING OF GASES BY PARTICLE SUSPENSIONS

This research was undertaken to improve the quantitative understanding of the thermal and optical processes during the radiant heating of gas-particle mixtures. In previous studies, we developed methods to calculate the solar absorption by the particles and determine the heating rates and temperatures of the gas and particles. In FY 1987 we continued development of a cylindrical receiver model and initiated experimental work to study the operation of a complete receiver system. The goal is to understand the complex interactions involved in the absorption of sunlight by the particles, the heating and expansion of the gas, and the resulting temperature, density, and flux profiles within a solar receiver. The results of the research will provide a basis to design future direct absorption receivers.

An analytical model of a long cylindrical receiver was developed to predict the temperature and flux distribution in a gas particle suspension flowing along its axis. The model uses a four-flux radiant transfer approximation that includes absorption, emission, and scattering by the particles, expansion of the gas, and convective and radiant heat transfer. The model provides general information regarding particle densities and the effects of flow direction. It also provides detailed performance predictions of our experimental receiver.

An experimental receiver system was designed and constructed to test the model. The experimental system consists of a vacuum-insulated cylindrical (.05 x 1 m) receiver, carbon particle generator, light source, and associated instrumentation. The light source produces a collimated beam of light along the axis of the tube with a peak intensity of over 80 suns. Carbon particles produced by the pyrolysis of C_2H_2 are mixed with air and directed in either a co- or counter-current flow direction with respect to the direction of the incident light. Thermocouples measure the temperature profile along the entire axis at 6 different radial positions and at fixed points within the receiver. The mixture opacity is monitored with laser transmissometers at 3 axial positions, and the total flux reaching the end is monitored. The receiver will be completed in FY 1988 and the measurements will be compared with the model predictions.

CARBON PARTICLE ABSORBERS IN LIQUID SALTS

The DOE Central Receiver Program is developing an advanced direct absorption receiver based on a liquid nitrate salt heat transfer and storage medium. The salt flows over a plate exposed to concentrated solar radiation from a field of heliostats. Because the pure salt is transparent to solar radiation, current designs call for the salt to be doped

*This work was supported by the Assistant Secretary for Conservation and Renewable Energy, Office of Systems Research, Energy Storage Division through the Solar Energy Research Institute, Sandia National Laboratories, and Battelle Pacific Northwest Laboratory, through the U.S. Department of Energy under Contract DE-AC03-76SF00098.

with cobalt oxide particles. In this second solar thermal concept we are investigating the use of carbon particles as an alternative absorber. Carbon particles are less abrasive and are slowly oxidized in the hot salt. The oxidation of the particles effectively eliminates problems of agglomeration and settling encountered with the cobalt oxide particles.

The study investigated the dispersion and oxidation of carbon particles in liquid Na/K nitrate salt. Experiments were run on 11 different types of carbon to study the ease of dispersal and the time to complete oxidation. Spectroscopic analysis of the salt after the experiments indicated that the carbon was oxidized to carbon monoxide, reducing the formation of undesirable nitrites. The carbon takes typically up to one hour to oxidize, meaning the rate of CO release to the air is very slow.

In addition to the experimental work, calculations were performed using a solar absorption model based on the Mie theory of scattering to determine the mass loading of carbon and cobalt oxide required to produce the necessary absorption in a path length of a few millimeters. These calculations showed that carbon was a better absorber on a weight basis than cobalt oxide. The work will continue in FY 1988 with a technical and economic assessment of the merits of the two absorbing agents.

RADIANTLY HEATED CATALYSTS FOR THERMOCHEMICAL ENERGY STORAGE

This work investigates the use of concentrated sunlight to directly initiate endothermic catalytic reactions in gases. This approach has application to high-temperature energy storage cycles using thermochemical reactions. Direct radiant heating of catalyst particles to drive endothermic reactions in gases offers significant advantages over traditional catalyst heating methods. These advantages include enhanced heat transfer because the heat is supplied directly to the site of the reaction. In conventional catalytic reactors, heat is supplied through pipe walls and to the reaction site by conduction and convection, leaving the catalyst the coolest part of the system. When a light-absorbing catalyst is radiantly heated it is the hottest part of the reactor, dramatically increasing the rate of reaction. Secondly, a semiconducting particle may photocatalyze the reaction because photons absorbed in semiconducting particles can produce energetic photocharges. In small particles these charges can reach the gases adsorbed on the surface and participate in the reaction.

We have studied the endothermic dissociation of SO_3 to SO_2 and O_2 as a vehicle for thermochemical storage of solar energy. This reaction occurs over a catalyst at 800 to 900°C. Experiments with hematite (iron oxide) particles fixed on a substrate and illuminated with a solar simulator showed large enhancements in dissociation rate. However, the SO_3 storage and transfer system was difficult to maintain because of the reactivity of the sulfur compounds. In addition, the reaction cell design caused uncertainty in the interpretation of the results. This year the SO_3 storage and transfer system was competely redesigned. A new reaction cell will be fabricated and the system assembled in FY 1988 for a new series of experiments.

RADIANTLY HEATED CATALYSTS FOR ENERGY TRANSPORT

A project was initiated to study the feasibility of direct radiant reactors for the chemical transport of energy. In this concept, parabolic dishes individually concentrate solar energy that is converted to chemical energy and piped as an energy-rich gas to a central site. The gases then pass over a catalyst to produce high-temperature heat to drive a steam-Rankine cycle. A similar process can also be used with central-receiver technology to transport energy for considerable distances. This approach is being explored in collaborative programs with Germany and Israel.

We are studying the feasibility of several types of direct radiant reactors for the CO_2 reforming of methane. CO_2 is reacted with methane over a catalyst at high temperature to produce H_2 and CO. Heat exchangers cool the gas to ambient temperature before it is piped to a central conversion site. Our investigation is analyzing several types of radiantly heated catalytic reactors with respect to operating characteristics and costs.

In all the receiver/reactor designs considered, solar flux was concentrated directly onto a catalyst immersed in the reacting gases. The catalyst was either arrayed on a non-absorbing substrate, or was entrained in the gas. The substrates considered included reticulated alumina, alumina aerogel, and fiber arrays. The fixed catalyst was chosen to be rhodium particles, which if very small become good solar absorbers. Analyses were carried out of the mass transport, optical and thermal properties of the reactor designs.

To aid in comparing the receiver designs, we developed a system model to study the first and second law efficiencies of the entire system.

PLANNED ACTIVITIES FOR FY 1988

Specific goals of the FY 1988 research include experimental validation of the gas-particle receiver model; characterization of the optical properties as well as the oxidation, agglomeration and settling of carbon particles in salt; quantification of the effects of radiant heating on the reaction rate of the dissociation of SO_3; and the development of integrated optical and thermochemical models of radiantly heated catalysts and their supports.

REFERENCES

1. Hunt, A.J., Ayer, J., Hull, P, Miller, F., Noring, J.E., and Worth, D., (1986), "Solar Radiant Heating of Gas-Particle Mixtures," Final Report, FY 1985 and FY 1986, LBL-22743.
2. Hunt, A.J. (1986), "New Approaches to Receiver Design," Proc. of the Third International Workshop, Konstanz, W. Germany.
3. Hunt, A.J. (1987), "Direct Absorption Receivers using Particle Suspensions," Proc. 3rd Meeting of SSPS Task III Group, Albuquerque, NM.

Microstructured Materials*

A. Hunt, F. Hibbler, P. Hsuin, and K. Lofftus

The goal of this work is to develop new microstructured materials using purely chemical techniques. Liquid organo-metallic compounds are combined with water, solvents, and catalysts to form a gel network that contains solvent. The solvent is removed without changing the microstructure by using a supercritical drying technique developed at LBL. The result is a low-density, porous solid called aerogel. A variety of single- or mixed-oxide compositions can be made this way depending on the starting compounds. Two projects are exploring this technique; one is developing silica aerogel for insulating windows, and the other is exploring the preparation of new ceramic materials.

ACCOMPLISHMENTS DURING FY 1987

SILICA AEROGEL, A TRANSPARENT HIGH-PERFORMANCE INSULATOR

Silica aerogel is a transparent, porous solid that is useful for a wide variety of applications. We are developing silica aerogel as a transparent insulator between double glazings for a high-thermal-performance window or solar collector cover. Such windows will increase the thermal resistance of conventional double glazing by a factor of 5 or more. Recent progress in improving the properties of silica aerogel, and the results of scale-up and technology-transfer activities are described.

Light passes through aerogel with essentially no distortion, but its microstructure scatters a small amount of blue light. We have been working to reduce this residual scattering to the point of acceptability for view glazings. Extensive experiments were carried out in the preparation of alcogel (the aerogel precursor) to determine the clearest formulation. A polarization nephelometer was used to quantify the light scattering from the alcogels. A rather remarkable result of the study was that, within the compositions investigated, the clarity was strongly correlated to the time to gellation.[1] The optimum aerogel density and catalyst content (over the range investigated) was determined to minimize scattering.

A new large autoclave capable of accommodating samples as large 12 inches square was designed and fabricated to carry out the CO_2 substitution and supercritical drying process developed at LBL. Instrumentation for monitoring the fluid level and composition in the autoclave was developed and tested. The first aerogel samples will be dried in the larger autoclave during FY 1988.

Cost studies were carried out that confirmed that aerogel could be produced for a reasonable cost ($10-15/m^2). The energy savings from using aerogel provide cost paybacks in less than two years in cold climates. Encouraged by the DOE technology transfer program, a company was founded to commercialize the manufacture of aerogel products in the United States using the CO_2 substitution process.

*This work was supported by the Assistant Secretary for Conservation and Renewable Energy, Office of Solar Heat Technologies, Solar Buildings Division, and the Office of Energy Systems Research, Energy Conversion and Utilization Technologies (ECUT) Division of the U.S. Department of Energy under Contract DE-AC03-76SF00098.

POROUS MICROMATERIALS DEVELOPMENT

Micromaterials research at LBL is developing new methods to produce microporous materials and precursors based on sol-gel chemistry and supercritical solvent extraction techniques. These techniques have enabled us to create new and unusual materials. Low-density materials with controlled microporosity promise applications including high-temperature insulators, ceramic precursors, and porous materials for filters, membranes, and catalyst substrates.

During FY 1987 we developed preparation methods for single and mixed oxide ceramic materials, initiated research into using sol-gel processing for preparation of high-T_c superconductors, and explored the preparation of organic gels. We studied the colloid chemistry involved in combining sols of alumina with silica. An aerogel with a composition corresponding to mullite (a widely used high-temperature ceramic) was prepared. Sintering tests showed that mullite aerogels sintered at significantly lower temperatures than conventional ceramic processing.[3] This is an important advantage in preparing ceramic composites because the components often react with each other at normal sintering temperatures. In addition to lowering sintering temperatures, the ultrafine aerogel microstructure results in a homogeneous material to near atomic scale.

After an extensive experimental search, we discovered a technique to prepare zirconia alcogels useful for making high-temperature insulators and porous electrodes. We also explored the preparation of mixed ceramic oxides for high-T_c superconductors. As a first step, we explored transesterifacation methods to prepare liquid copper alkoxide starting compounds. YBa_2Cu_{7-x} aerogels may offer significant advantages because the lowered sintering temperature can avoid undesirable phase transitions encountered at normal processing temperatures and the porous structure allows easy oxygen transport.

PLANNED ACTIVITIES FOR 1988

In the silica aerogel research we will concentrate on producing large aerogel tiles for evaluation by industry and encourage the commercial development of aerogel windows and skylights through technology transfer activities. The porous micromaterials area will explore the preparation of transparent dense alumina by sintering aerogel precursors, continue to develop preparation methods for zirconia aerogels, and explore the preparation of copper and mixed-oxide aerogels for high-T_c superconductors.

REFERENCES

1. Hunt, A.J. and Lofftus, K. (1987), "Silica Aerogel, A Transparent High Performance Insulator," Proc. of the International Solar Energy Society World Congress, Hamburg, Germany.
2. Hunt, A.J. and Lofftus, K. (1986), "Porous Micromaterials Development," LBL-22811.
3. Rahamam, M.N., DeJonghe, L.C., Shinde, S., and Tewari, P.H. (1987), "Sintering and Microstructure of Mullite Aerogels," submitted to *J. Am. Ceramic Soc.*, LBL-23529.

Light Scattering Studies*

As part of the study of the interaction of light with microstructures, we have established a capability to carry out basic studies of light scattering. Light scattering is an essential tool in our solar thermal conversion and microstructured materials studies. We are also investigating two topics in the biological sciences. Both involve the detection of specific and unusual effects of scattered light in either live populations or immobilized single cells.

*This work was supported by the National Institutes of Health through the National Heart, Lung and Blood Institute, and the Environmental Sciences Programs Directorate of the Office of Naval Research, through the U.S. Department of Energy under Contract DE-AC03-76SF00098.

ACCOMPLISHMENTS DURING FY 1987

OPTICAL MEASUREMENTS OF THE INTRACELLULAR POLYMERIZATION OF HbS

A. Hunt, C. Gross, K. Lofftus, and A. Quintanilha

A new, real-time technique we have developed measures the kinetics of intracellular polymerization of sickle cell hemoglobin. Previously, it was difficult to distinguish polymerization from shape changes in the cell and to quantify polymerization caused by de-oxygenation, hypertonic stress, acidification, or temperature increase. Time-dependent measurements

of the effects of these stresses are important because kinetics plays a key role in the physiological processes that lead to crises in sickle cell patients. We have shown that measurements using a polarization-sensitive light-scattering technique[1] can detect and quantify hemoglobin polymerization.[2] Further, the technique clearly distinguishes polymerization from changes induced in the shape or volume of the cells. The technique is extremely sensitive, allowing studies with very small sample volumes, an important advantage when working with sickle blood.

In a series of measurements on blood of juvenile sickle patients, the normalized induced circular polarized light, measured as a function of angle, changed by 1.5% in a reversible manner when the O_2 content alternatively varied from 7.5 to 0.5 ppm. The current instrumental resolution is about 0.2%. Further, blood from non-sickle patients showed no change within experimental uncertainty under similar experimental conditions. We are currently using this technique to study the kinetics of sickling behavior and how it correlates to perturbations of membrane transport phenomena.

MODELING BIOLOGICAL PARTICLES TO PREDICT OPTICAL PROPERTIES OF THE OCEAN

A. Hunt, M. Quinby-Hunt, F. Livolant, K. Lofftus, and M. Maestre

The objective of this project, begun in June of 1987, is to predict the scattering behavior of the ocean through a modeling program and to evaluate the effects of that scattering on oceanic visibility and irradiance. The largest and most variable component of oceanic scattering arises from particles suspended in the ocean. The organisms can be identified as members of groups, which are *self-similar* and can be described as simple geometric forms or combinations of them. Therefore, it is possible to predict the scattering from such organisms by applying one or more scattering theories depending on the size, internal and external structure, refractive index, and absorptive properties of the organism.[3]

A series of models was implemented as computer programs to predict scattering from a variety of structured particles. For marine organisms with spherical symmetry, rigorous calculations can be performed for unrestricted size and optical properties using Mie theory. Models based on Rayleigh-Debye theory are valid only for a restricted range of sizes and optical properties but predict scattering for a variety of shapes. Computer programs were developed to determine the range of validity of the non-rigorous theories by comparison with rigorous theories for spherical geometries.

A new method was developed for measuring the optical properties of single, immobilized marine organisms. Fixed cells[4] of the dinoflagellate *Prorocentrum micans* were immobilized in a transparent silica gel. Because the solvent in the gel dominates the relative refractive index, the residual scattering caused by the gel can be effectively eliminated. The technique provides a convenient method to perform scattering or other optical measurements on immobilized cells without interference of a substrate in a liquid medium.

PLANNED ACCOMPLISHMENTS FOR FY 1988

Measurements of the sickling behavior of HbS will be expanded to determine the kinetics and quantify the differences in density-gradient-separated red cell populations.

Models will be developed comparing the unrestricted Mie calculations and Rayleigh-Debye approximations for the infinite cylinder. Rayleigh-Debye theory will be used to model more-complex-shaped particles. Preliminary measurements of *Prorocentrum Micans* performed this year revealed an unexpectedly strong circular polarization signal. These measurements will be repeated in FY 1988 with improved equipment and in greater detail.

REFERENCES

1. Hunt A.J. and Huffman, D.R. (1973), "A New Polarization-Modulation Light Scattering Instrument," *Rev. Sci. Instr. 44,* 1753.
2. Hunt, A.J., Lofftus, K.L., and Quintanilha, A. (1987), "Optical Measurements of the Intracellular Polymerization of HbS," *Blood, (J. Am. Soc. Hematology) 70, No. 5,* 62a.
3. Quinby-Hunt, M.S., Hunt, A.J. and Brady, S.A. (1986), "Polarization-modulation Scattering Measurements of Well-Characterized Marine Plankton," *SPIE, Ocean Optics VIII, 637,* 155.
4. Livolant, These de Doctorat D'Etat, Univ. Pierre et Marie Curie (Paris).

Solid-State Radiative Heat Pump*

P. Berdahl

The objective of this project is to establish the research basis for the development of a new class of heat pump. This new heat pump will be a solid-state device that accepts input energy in the form of electricity and pumps infrared (heat) radiation across a thermally insulating gap. An important potential application is the heating and cooling of buildings, including applications using thermal storage.

Semiconductor materials with direct narrow bandgaps in the range of 0.03-0.25 eV emit equilibrium thermal radiation which is in large part due to electron-hole recombination. An excess or deficit of infrared radiation, compared to the thermal equilibrium value, can be produced when the concentrations of electrons and holes are varied from their thermal equilibrium values by electrical means. Two techniques for varying the concentrations of electrons and holes are of special interest here: (1) electrical bias of a p-n junction to produce carrier injection or, for reverse bias, carrier extraction; (2) the magneto-concentration effect in which orthogonal electric and magnetic fields are used to enhance (or deplete) the concentrations of electrons and holes near the semiconductor's surface. The p-n junction technique seems particularly promising for the development of technologically mature devices, while the magneto-concentration effect offers the opportunity for the study of key recombination phenomena in a simpler experimental system.

Recently, the magneto-concentration effect was employed to explicitly demonstrate a galvanomagnetic radiative cooling effect.[1] This experiment proved that working solid-state radiative heat pumps can be constructed. However, increases in efficiency are required for this technology to compete with more conventional heating and cooling techniques.

ACCOMPLISHMENTS DURING FY 1987

Ongoing measurements of the quantum efficiency of radiative recombination in InSb were continued in order to clarify the values that this key sub-efficiency can take and to determine whether or not this efficiency can be improved by doping, as suggested by theoretical considerations. Figure 1

*This work was supported by the Assistant Secretary for Conservation and Renewable Energy, Office of Energy Storage and Distribution of the U.S. Department of Energy under Contract No. DE-AC03-76SF00098.

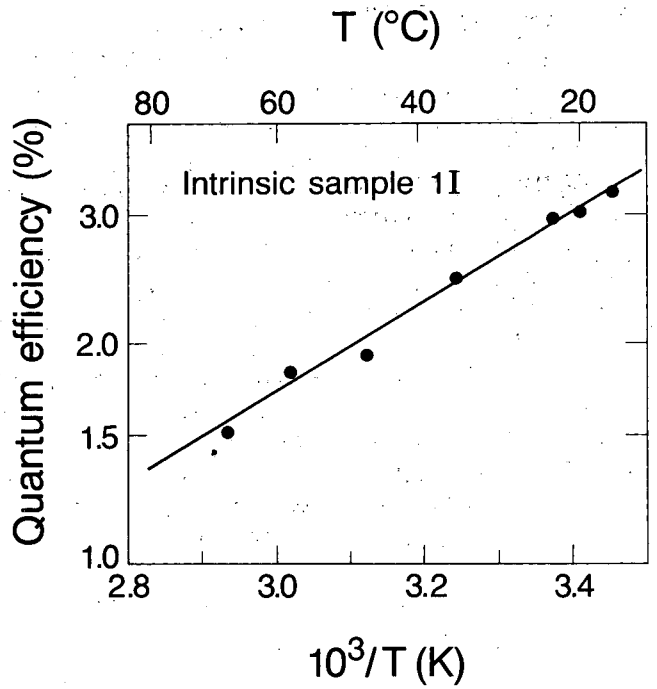

Figure 1.. Measured quantum efficiency of radiative recombination (logarithmic scale), in a pure sample of InSb, as a function of temperature. The solid line is a fit to the data. (XBL 873-6243)

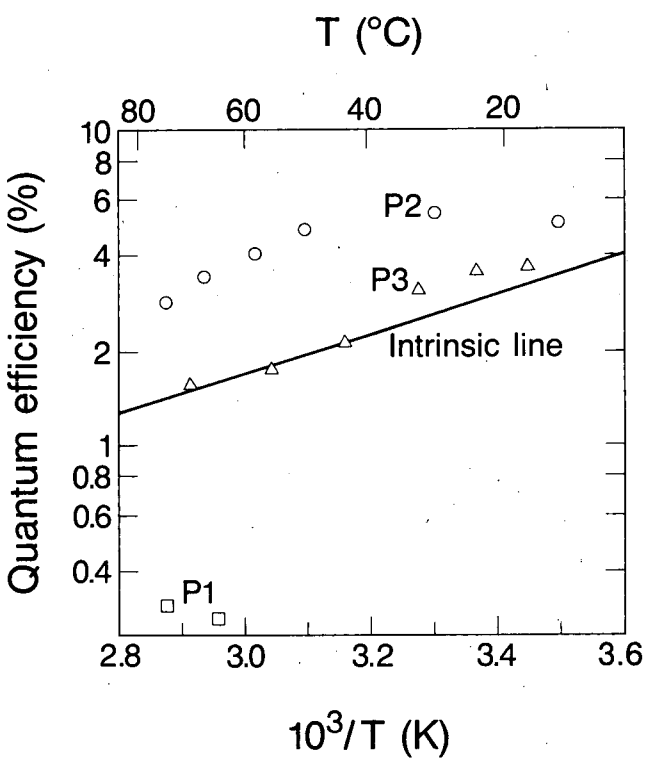

Figure 2. Measured quantum efficiencies for radiative recombination. The solid line is from Fig. 1. The doping (impurity) concentration, in units of 10^{16} cm^{-3}, is 4.2 for sample P3, 25 for sample P2, and 140 for sample P1. (XBL 873-6246)

shows measured values of the quantum efficiency of radiative recombination in pure (intrinsic) InSb as a function of temperature, as measured using our galvanomagnetic luminescence technique.[2] The efficiency is 3% at room temperature, too low to form the basis of a highly efficient heat pump. However, Fig. 2 shows that the addition of p-type impurities (cadmium atoms in this case) can raise the quantum efficiency to values at least as high as 5%. The detailed interpretation of these results [3] is that p-type impurity atoms suppress the dominant form of non-radiative recombination (the Auger mechanism), and therefore enhance the importance of radiative processes. The Cd impurities also introduce new non-radiative recombination processes, so there is an optimum level of doping, with an impurity concentration of roughly 2×10^{17} atoms cm^{-3}.

PLANNED ACTIVITIES FOR FY 1988

Further research on InSb is desired and may be expected to raise the quantum efficiency for radiative recombination even further. However, it is important to begin the evaluation of other promising narrow-bandgap semiconductor materials, such as the lead-tin-tellurides, to determine their suitability for applications in solid-state radiative heat pumps. Therefore future research will include studies of radiative recombination with these unexplored materials.

REFERENCES

1. Berdahl, P. (1987), *Proc. 18th Int. Conf. on the Physics of Semiconductors,* Stockholm, 1595.
2. Berdahl, P. and Shaffer, L. (1985), *Appl. Phys. Lett. 47,* 1330.
3. Berdahl, P. (1987), *J. Appl. Phys.* (In press). LBL-23234.

COAL-RELATED RESEARCH

Processing of Condensate Waters from Coal Gasification*

C.J. King, J. Senetar, T. Grant, L. Poole, and R. Thompson

Condensate waters from low-temperature coal-gasification processes contain large concentrations of ammonia, acid gases, and dissolved organics – notably phenolic compounds. For both economic and environmental reasons it is necessary to purify these waters sufficiently to allow recycle, probably as make-up to a cooling-tower system. The principal objective of this project has been to provide basic understanding enabling improved solvent-extraction, adsorption, and stripping processes for these condensate waters. Current research focuses upon removal of organics by regenerated carbon adsorption processes, and development of a more energy-efficient approach for recovery of ammonia.

Use of carbon adsorption for condensate waters is held back by incomplete regeneration of the carbon, which typically requires replenishment of 15% or more of the carbon per cycle. Our goal is to identify the cause of this irreversibility and to develop means of overcoming or lessening the problem.

Stripping of ammonia from condensate waters is energy-intensive, because the volatility of ammonia is lowered by the presence of dissolved acids, notably carbon dioxide and hydrogen sulfide. We have pursued an improved approach, wherein ammonia is extracted with a liquid ion exchanger, while the acid gases are simultaneously stripped. This greatly reduces the steam requirement for stripping and serves to isolate ammonia as a product.

ACCOMPLISHMENTS DURING FY 1987

Adsorption of Phenols

Through several complementary experimental approaches we have confirmed that phenols undergo a slow chemical reaction with carbon surfaces. The reaction is apparently irreversible, leading to higher molecular-weight products, which we have been able to identify by liquid chromatography of leachates. Solvent regeneration by liquid extraction is more efficient than regeneration by heating and vaporization. Several common solvents give nearly complete recovery of unreacted adsorbed phenols.

Isolation and Recovery of Ammonia

We have shown that organophosphinic acids have optimum basicity for extracting ammonia from condensate waters (favored by high basicity) with efficient regeneration by distillation of ammonia (favored by low basicity). We have developed a means of purifying Cyanex 272, a commercial phosphinic acid extractant, and have used the purified extractant to determine and interpret extraction equilibria and regenerability.

PLANNED ACTIVITIES FOR FY 1988

Adsorption of Phenols by Carbon

We are observing reaction kinetics for different phenolic solutes as they react with carbons having different surface characteristics, so as to define the chemistry of the reaction between phenols and carbons. This information is used to identify processing approaches which minimize irreversibility and hence minimize carbon consumption.

Extraction of Ammonia

We are carrying out experiments with purified Cyanex 272 to characterize the amount of increased aqueous solubility and/or increased vapor pressure of hydrocarbon decomposition products resulting from heating during distillation. Since process efficiency is increased by carrying out the distillation of ammonia from the extractant at higher temperatures, the temperature limit for thermal degradation determines the overall efficiency of the extractive approach for ammonia recovery.

*This work was supported by the Program Development Funds through the U.S. Department of Energy under Contract No. DE-AC03-76SF00098.

Removal of H_2S from Coal-Derived Gases*

S. Lynn, R. Hix, D. Neumann, S. Sciamanna, and C. Stevens

When coal is gasified most of the sulfur is converted to H_2S and must be removed before the gas can be used either as a fuel or as synthesis gas. The UCB Sulfur Recovery Process (UCBSRP) is being developed as a general method for removing H_2S from gases. The H_2S is absorbed in a polyglycol ether, then reacted in the liquid phase with SO_2 to form marketable elemental sulfur and water. The process allows high specificity and flexibility; H_2S can be reduced to the part-per-million level or below in the presence of CO_2 and the other components of gasified coal. The CO_2 may be left in the original gas stream or it may be co-absorbed and recovered as a separate, sulfur-free product. The process thus has application both to syngas and hydrogen production from O_2-blown gasifiers and to power production using an air-blown gasifier.

ACCOMPLISHMENTS DURING FY 1987

Process Configuration Studies

Figure 1 shows a flowsheet for the UCBSRP in a configuration that gives maximum selectivity for H_2S removal. In the primary absorber H_2S is removed principally by physical absorption. The stream of solvent leaving the absorber is nearly saturated with all of the components of the gas being treated. A water wash at the top of the primary absorber prevents loss of solvent vapor in the treated gas.

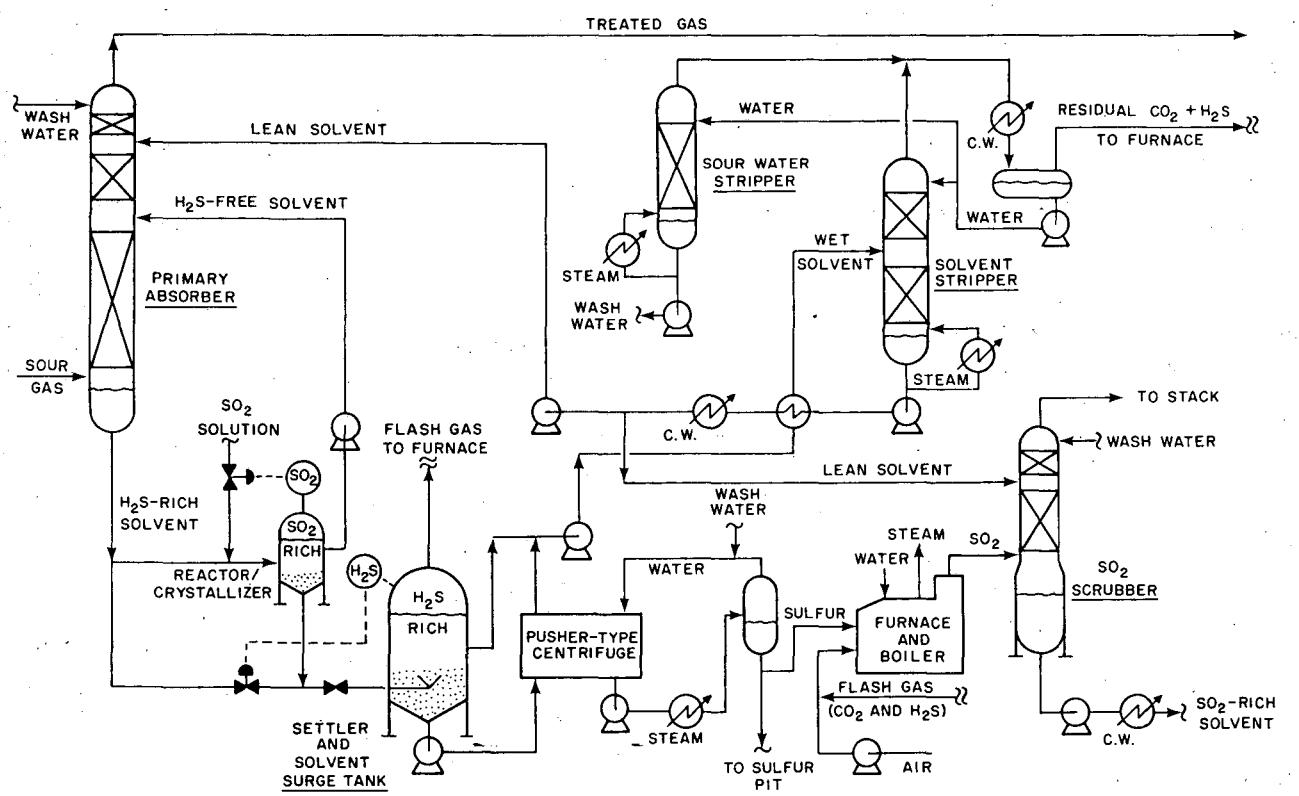

Figure 1. UCB Sulfur Recovery Process–process configuration for high H_2S selectivity. (XBL 882-583)

*This work was supported by the Assistant Secretary for Fossil Energy, Office of Coal Utilization, Division of Surface Coal Gasification of the U.S. Department of Energy under Contract No. DE-AC03-76SF00098.

Most of the solvent stream leaving the primary absorber then enters a reactor/crystallizer that operates at the pressure of the primary absorber. A second solvent stream containing SO_2 is metered into the same reactor at a rate that keeps the SO_2 content within the reactor a few percent above stoichiometric relative to the H_2S. (It is necessary to have an excess of one reactant or the other in each reactor to avoid excessive reactor volumes and the need for highly precise reactor control). A clarified overflow from the SO_2-rich reactor is pumped back to the primary absorber. This solvent stream has been completely freed of its H_2S content but is still saturated with respect to the other components in the gas being treated in the primary absorber. The net co-absorption of these other gas components (such as CO_2) is thus kept quite small and the effective selectivity for H_2S is of the order of 50 to 100. The SO_2 content of this solvent stream, although low, provides a chemical enhancement for the absorption of the H_2S on the upper trays of the primary absorber to facilitate meeting very stringent H_2S specifications in the treated gas. (The temperature in the primary absorber is high enough to prevent precipitation of the sulfur formed by this reaction. Not shown in Fig. 1, to avoid clutter, is provision for cooling both reactor/crystallizers with cooling water so that the solvent is sub-saturated in sulfur at all other points in the system).

The underflow from the SO_2-rich reactor carries the sulfur and water formed in the reaction between H_2S and SO_2. The flow of this stream is sized to keep the water content of the solvent from exceeding 5% and is directly proportional to the rate of H_2S removal – the flow will typically be about 10% of the total flow of solvent through the primary absorber. Sufficient H_2S-rich solvent, from the primary absorber, is added to the stream to leave a small excess of H_2S after all of the residual SO_2 has reacted. This stream is then flashed to atmospheric pressure in the settler/surge tank.

The sulfur made in the process forms a slurry in the underflow from the surge tank. The sulfur is recovered and washed in a centrifuge. In most cases about one-third of the sulfur will be burned in the furnace to make the SO_2 needed in the process. The energy recovered in the waste-heat boiler will usually supply and perhaps exceed the energy required by the process.

The overflow streams from the surge tank and the centrifuge are combined and sent to the solvent stripper. Boiling most of the water out of the solvent provides a stripping vapor that also removes unreacted H_2S and co-absorbed gases such as CO_2 from the solvent. Most of the solvent leaving the solvent stripper is used in the SO_2 scrubber where it absorbs the SO_2 from the combustion gas leaving the furnace. The SO_2 content of this solvent is nil, and hence the SO_2 content of the stack gas leaving the scrubber can readily be reduced to the part-per-million level. The remainder of the solvent from the stripper is sent to the primary absorber, where it prevents loss of SO_2 in the treated gas.

Figure 2 shows a process configuration suitable for removing and recovering one or more components (in addition to the H_2S) from the gas being treated, such as removing CO_2 from a synthesis gas ahead of a shift reactor in a process for producing hydrogen. The operation of this process is identical to that described above in many respects. It differs as follows: the H_2 and CO are stripped from the solvent. The stripping gas is obtained by a partial flash of the solvent immediately downstream of the primary absorber. Most of the H_2S-rich solvent stream leaving the flash drum, together with a controlled flow of SO_2 solution, enters an SO_2-rich reactor. The pressure of the SO_2-rich solvent stream is reduced in stages (only two are shown) to about one atmosphere. The off-gas from each stage is recompressed to the pressure desired for the CO_2 product and is contacted with neat solvent to remove traces of SO_2, then washed with water to recover solvent vapor. For the case shown, in which a high degree of CO_2 removal is not required, clarified H_2S-free solvent from the atmospheric flash can be pumped directly back to the primary absorber.

As in the flow configuration designed for high H_2S selectivity, the sulfur and water formed in the reaction are conveyed out of the last SO_2-rich reactor in a stream that is rendered H_2S-rich with by-passed H_2S solution. As before, the flow of this stream is proportional to the rate of sulfur production.

Corrosion Studies

Corrosion studies were performed by submerging metal coupons half way in a solution of H_2S or SO_2 in a glycol ether. To make the system as corrosive as possible, the solvent was a mono-ether (which is also an alcohol) and sulfur and water were added in concentrations twice (or greater) those encountered in the process. The exposure was carried out for three successive 20- to 30-day periods at each temperature. Table 1 shows the corrosion rates observed. Since 60°C is the maximum temperature at which SO_2 is present (outlet of the SO_2 absorber), carbon steel and 304 and 316 stainless steels should corrode at rates much less than 1 mil/year (0.02 mm/yr) under all process conditions.

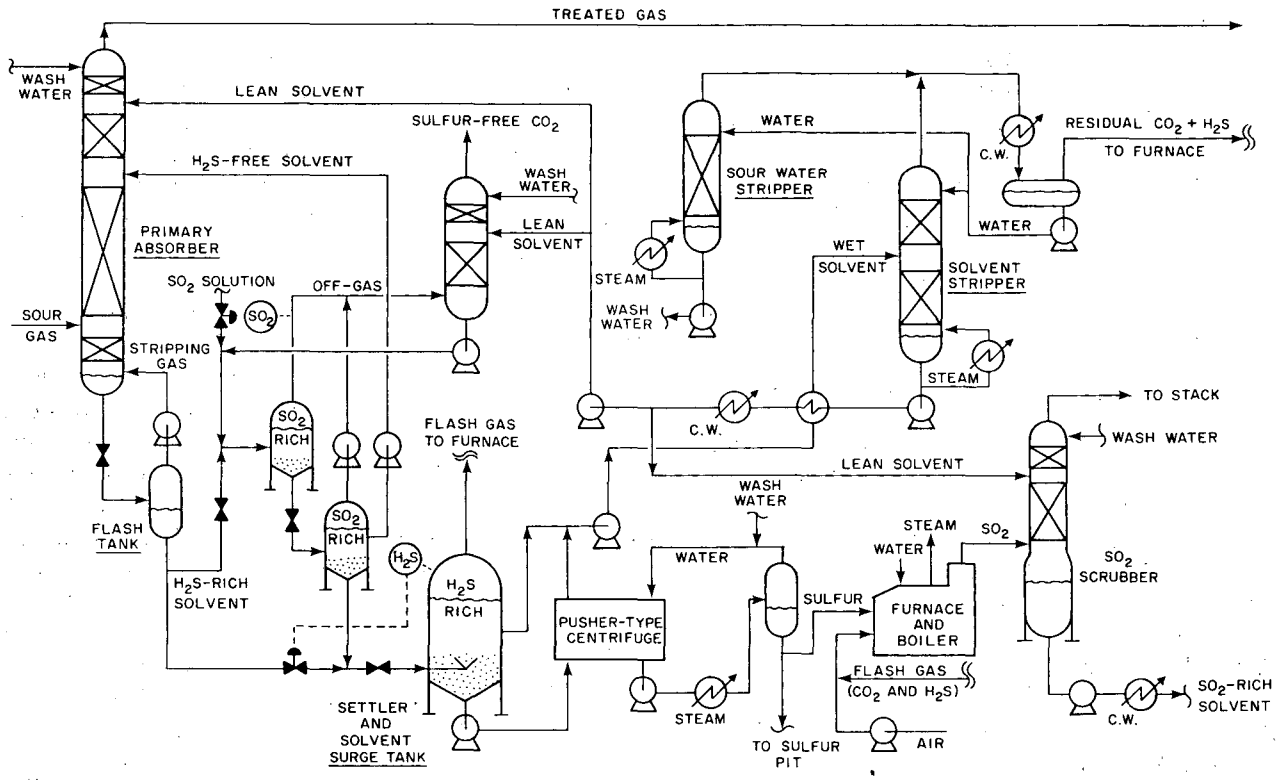

Figure 2. UCB Sulfur Recovery Process–process configuration for co-absorption of CO_2. (XBL 882-582)

Sulfur Crystallization

A major potential advantage of the UCB Sulfur Recovery Process is the purity of the crystalline sulfur that is produced. The sulfur crystallizes from solution both as a result of cooling and as a result of chemical reaction between H_2S and SO_2. In the former case the degree of supersaturation is relatively low because the solubility of sulfur in the solvent varies only a few grams per liter over the temperature range of interest. A substantially higher concentration of sulfur can result from the chemical reaction.

The crystallizer consists of a well-stirred 2-liter vessel. Hot saturated feed enters at the top, and the vessel walls are cooled. Cold effluent exits at the bottom of the vessel as a sulfur/solvent slurry. A sample of the effluent slurry is collected when the system is at steady-state and the size distribution of the sulfur crystals is determined.

Table 1. Corrosion Rates of Steels in Process Solutions.

	MEASURED RATES AND CONDITIONS *		
Metal	SO_2: @ 100°C	@ 120°C	H_2S: @ 150°C
Carbon Steel	0.6	1.7	0.05
304 Stainless	0.7	1.5	0.02
316 Stainless	1.3	4.8	0.01

* Mils/year in diethylene glycol methyl ether, 5% H_2O, saturated with sulfur, 50 - 100 psi gas pressure.

Gas Absorption with Chemical Reaction

Tray efficiency data are needed for two process situations. In one, H_2S at very low concentration is being absorbed by a chemically reactive solution of SO_2. In the other, gaseous SO_2 in the low parts-per-million concentration range is absorbed by lean process solvent. Both are of interest because one wishes to effect very stringent sulfur removal with the UCBSRP. The equipment consists of a single sieve tray (or section of packed column) placed in a test section through which gas and liquid streams pass. Murphree tray efficiencies are determined from the mass balances and previously obtained solubility data.

PLANNED ACTIVITIES FOR FY 1988

The crystallizer is being modified to incorporate crystal size classification to retain smaller crystals and produce a product of larger size. Sulfur will be produced by chemical reaction. Data obtained for absorption of H_2S enhanced by the presence of SO_2 in the solvent will be used to develop a model that incorporates the reaction kinetics work done previously.

A computer model that simulates all of the unit operations in the process is operational and facilitates process synthesis for specific applications. It will be used to evaluate and further refine the process configurations shown in Figs. 1 and 2 for the purification of hydrogen derived from gasified coal.

PUBLICATIONS

1. Demyanovich, R.J. and Lynn, S. (1987). "Vapor-Liquid Equilibria of Sulfur Dioxide in Polar Organic Solvents," *I&EC Research 26,* 548.

2. Lynn, S., Neumann, D.W., Sciamanna, S.F., and Vorhis, F.H. (1987), "A Comparison of the UCB Sulfur Recovery Process with Conventional Sulfur Recovery Technology," *Environmental Progress 6,* 257.

3. Neumann, D.W. and Lynn, S. (1986), "Kinetics of the Reaction of H_2S and SO_2 in Organic Solvents," *I&EC Proc. Des. & Dev. 25,* 248.

Analysis of Coal Gasification Reactors*

M.M. Denn and G. Dow

This research project is concerned with modeling moving-bed coal gasifiers in order to gain insight into reactor operability and design. Detailed single-particle models seem to provide the most realistic description of the transport phenomena and chemical kinetics near the coal surface. Rather than modeling the complete reactor as a continuum of individual particles, we describe the flow pathway of the gases through the coal bed as a plane channel whose sides are composed of reactive carbon. This pore model of the gasifier incorporates a detailed description of the coal surface which implicitly accounts for particle-particle interactions.

ACCOMPLISHMENTS DURING FY 1987

An automatic remeshing scheme has been incorporated into our numerical method for solving the model equations. With a fixed number of nodes, this scheme adjusts the finite-difference mesh so that the nodes are concentrated in the region where rapid combustion of carbon generates steep temperature and composition gradients.

We have adapted our model to study the influence of gas-phase oxidation, solid-gas temperature differences, and transverse gradients on predictions of reactor performance. The consideration of these factors as well as the description of the coal surface serves to categorize current modeling efforts.[1]

Figure 1 shows the gas temperature profiles predicted for typical operating conditions in an air-blown Lurgi gasifier. The inclusion of differing solid and gas temperatures lowers the peak temperature and pushes the hot spot closer to the gas feed.

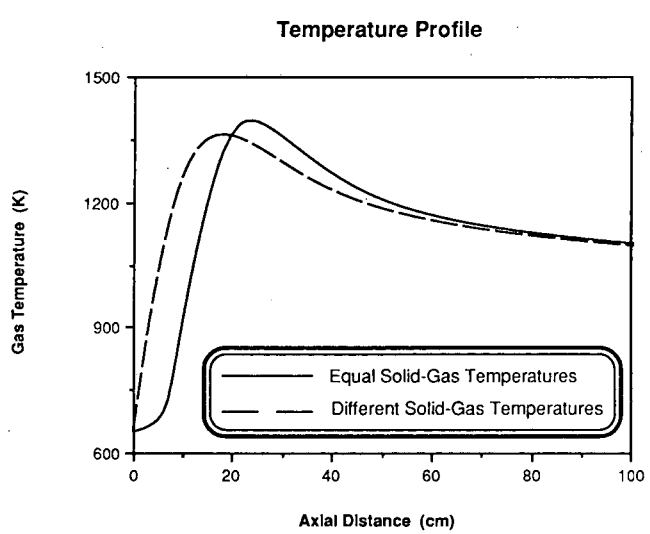

Figure 1. Gas temperature profiles for a one-dimensional channel model of a moving-bed gasifier. (XBL 882-575)

*This work was supported by the Morgantown Energy Technology Center, Assistant Secretary for Fossil Energy, Office of Coal Utilization, Advanced Research and Technology Development, Division of Surface Coal Gasification through the U.S. Department of Energy under Contract No. DE-AC03-76SF00098.

PLANNED ACTIVITIES FOR FY 1988

The study will be completed in FY88. We will explore how operating conditions such as blast temperature and reactant feed rates affect reactor performance.

REFERENCE

1. Denn, M.M. and R. Shinnar (1987), "Coal Gasification Reactors," in J.J. Carberry and A. Varma, eds., *Chemical Reaction and Reactor Engineering,* Marcel Dekker.

Energy-Related Organometallic Chemistry*

The work in this area is described in the following four sections.

BIOMIMETIC ORGANOMETALLIC CHEMISTRY

R.H. Fish and R.T. Price

The recent interest in the synthesis of biomimetic catalysts that mimic the biologically important cytochrome P-450 dependent monooxygenase enzyme reaction[1-3] by converting C-H bonds to C-OH bonds in a regio- and stereoselective manner has led to an enormous number of contributions that have clearly shown similar reactivity to the reactive metal center of that enzyme.[4-6] While the types of substrates that have been studied with these biomimics have included alkanes and alkenes, it was surprising, therefore, to discover that no examples of organometallic substrates have been reported with these biomimetic catalysts.

One class of organometallic compounds, the organotins, have been shown to have a wide variety of biological activity[7] and have been studied in depth with a cytochrome P-450 enzyme system from rat liver microsomes.[8-13] Those studies were unequivocal in determining that the tin atom controlled the regiochemistry when substrate steric effects at the binding site in proximity to the active metal center were not a factor.[8,9] In addition, those studies clearly were among the first to assign a free radical mechanism to the P-450 enzyme in the conversion of C-H bonds to C-OH bonds, with the tin atom able to stabilize the intermediate carbon radicals that were alpha and beta to it.[8-11,14]

More importantly, we were also able to study, with the enzyme system, the regio- and stereoselective aspects of this conversion with cyclohexyltriphenyltin, **1**, and demonstrate that steric effects at the binding site in proximity to the active metal center control the regiochemistry. Thus, we have reported the first example of the use of an organometallic substrate, **1**, with "oxo" metalloporphyrins that have been shown to be biomimetic catalysts for the cytochrome P-450 active metal center, iron(III) or manganese(III) tetrakis(pentafluorophenyl)porphyrin derivatives $[TPF_5P(Br,OAc)]$[5] in the presence of the oxygen transfer agent, iodosylbenzene, and establish the regio- and stereoselectivity of the hydroxylation reaction, while comparing the results to those found for the enzyme system.

Accomplishments During FY87

The regio- and stereoselectivity in the hydroxylation reaction of cyclohexyltriphenyltin with biomimetic catalysts that mimic the important cytochrome P-450 monooxygenase enzymes, the iron(III) and manganese(III) tetrakis(pentafluorophenyl) porphyrin derivatives, was studied with the oxygen transfer agent, iodosylbenzene, and the results compared to those obtained for the enzyme. It was found that the regioselectivity on a per hydrogen basis for the biomimetic catalysts provided a C4:C3:C2:C1 ratio of 1:2:6:0 and a high stereoselectivity of equatorial to axial hydroxyl products, with a EQ/AX ratio of 29. The enzyme had a regioselectivity ratio with C4:C3:C2:C1 being 109:7:1:0 and a high EQ/AX ratio of 59. The dramatic regiochemical differences between the biomimic and the cytochrome P-450 monooxygenase enzyme can be explained by the fact that the enzyme provides steric constraints at the binding site in proximity to the active oxo metal center, while the biomimics we utilized did not have these constraints. The hydroxylation results with the biomimetic catalysts also suggests a free radical reaction, since the carbon-tin bond can stabilize intermediate carbon radicals and gave *trans*-2-hydroxycyclohexyltriphenyltin and *cis*-3-hydroxycyclohexyltriphenyltin as the major oxidation products. They also suggest a free radical cage effect, since we observed a high EQ/AX ratio and the absence of *cis*-2 and *cis*-4-hydroxycyclohexyltriphenyltin products.

Planned Activities for FY88

We plan to concentrate on the C-H activation of hydrocarbons with biomimetic catalysts.

*This work was supported by the Electric Power Research Institute; the Assistant Secretary for Fossil Energy, Office of Oil, Gas and Shale Technology, through the Bartlesville Project Office; and the Director, Office of Energy Research, Office of Basic Energy Science, Chemical Sciences Division, of the U.S. Department of Energy under Contract No. DE-AC03-76SF00098.

BIOMIMETIC CARBON-HYDROGEN ACTIVATION CHEMISTRY

R.H. Fish, R.T. Price, and R.H. Fong

The use of biomimetic catalysts that convert C-H bonds to C-OH bonds in the presence of an oxygen source is an area of intense research interest.[4-6] The enzyme that has been most important in the success of these biomimetic studies has been cytochrome P-450, which has been studied in-depth.[1-3] Recent findings have clearly shown that shape selectivity, built into the biomimics at the active metal center, is an important parameter for comparison of the regiochemical results of the mimics to those obtained with the P-450 enzyme.

More-recent reports have focused on supramolecule porphyrins[15-19] that contain a microenvironment more representative of the enzymes and these have been shown to be able to bind oxygen,[15] oxygenate olefins[19] and do C-H activation chemistry[20] with a monooxygen reagent. We were intrigued by the possibility that the supramolecule porphyrins would show any special reactivity in the carbon-hydrogen activation of their putative intermediate "oxo" derivatives with small hydrocarbons (C_1-C_3) to preferentially form the corresponding alcohols from those hydrocarbons. To our knowledge, this is the first reported attempt of C-H activation chemistry with C_1-C_3 hydrocarbons with a supramolecule metal porphyrin catalyst and allows an evaluation of the microenvironment surrounding the active metal center compared to an open-face porphyrin as well as kinetic and thermodynamic factors that control C-H activation.

Accomplishments During FY87

The manganese (III) complex of the doubly looped, superstructured amide ligand, **1**,[18] was evaluated in the C-H activation reactions of methane, ethane, propane and cyclohexane to provide the corresponding alcohols using iodosylbenzene as the monooxygen transfer agent. Table 1 compares the results using catalysts **1** and **2**, an open-face, meso-substituted manganese porphyrin, Mn(III)TF_5PP(OAc), to provide information on the C-H bond reactivity of the four hydrocarbons studied. This includes the yield of the product alcohol, ketone or chloride and the turnover number.

Planned Activities for FY88

Since our goal is C-H activation of methane and ethane to their respective alcohols, we are presently evaluating biomimetic porphyrin and non-porphyrin

Table 1: Carbon-Hydrogen Activation of Hydrocarbons Using Compounds **1** and **2** as Catalysts and Iodosylbenzene as the Monooxygen Transfer Agent.[a]

Hydrocarbon	Product (%)[b]		Turnover No.	
	1	2	1	2
CH_4	NPD[c]	NPD		
CH_3CH_3	CH_3CH_2OH (1)	CH_3CH_2OH (2.7)	0.23	0.54
$CH_3CH_2CH_3$	$(CH_3)_2CHOH$ (9.6)[d]	$(CH_3)_2CHOH$ (13.5)[e]	2.1	2.8
	$CH_3CH_2CH_2OH$ (0.6)	$CH_3CH_2CH_2OH$ (1)		
CycloC_6H_{12}	$C_6H_{11}OH$ (72)	$C_6H_{11}OH$ (69.4)	16.7	14.0
	$C_6H_{10}O$ (5.2)	$C_6H_{10}O$ (1)		
	$C_6H_{11}Cl$ (4.5)	NPD		

[a]Reactions of methane, ethane and propane were run in a Parr kinetic apparatus at room temperature for 24 h at 100-500 psi with a iodosylbenzene to catalyst ratio of 20:1. Catalyst concentration was at room temperature in Schlenk tubes with substrate: iodosylbenzene: catalyst ratios of 1100:20:1 in methylene chloride. Analysis and quantitation of products was obtained via capillary column GC analysis with a 15m • .035 mm DB5 column.
[b]Based on the mmoles of iodosylbenzene.
[c]No product detected.
[d]Ratio of 2° to 1° C-H bond reactivity on a per H basis is 45:1.
[e]Ratio is 42:1.

catalysts that have longer half-lives and better shape selectivity to overcome the thermodynamic disadvantage of an appreciable C-H bond dissociation energy and to hopefully provide a kinetic advantage for activation.

POLYMER PENDANT LIGAND CHEMISTRY, 2

R.H. Fish, A.D. Thormodsen, R.B. Belser, Jr., G. Friedman and J.G. Reynolds

The use of polymer pendant ligands to remove metal ions from solution is an area of intense research interest. The applications for facile metal ion removal with these pendant ligands are unlimited; however, in most of the reported applications the molecular structures of the metal compounds, both in the complex media in which they are present and those that are formed on the modified polymers, are not always clearly defined.

Thus, in this paper,[21] we report studies on the reactions of both 2% and 20% CAT-PS-DVB resins with $VO(AcAc)_2$ at various times and at equilibrium, as well as the diffusion limitations of increased cross-linking, and the effects of the base, triethylamine, and the bidentate ligand, bipyridine, on the equilibrium value for removal of vanadyl ion from solution. We have also addressed the structure of the vanadium complexes on the 20% CAT-PS-DVB resin by infrared and EPR spectroscopic techniques. As well, vanadium distributions for both the 2% and 20% CAT-PS-DVB resins were determined by SEM and EDX analysis.

Accomplishments During FY87

The reactions of catechol ligands, bonded to either 2% or 20% cross-linked methylated polystyrene-divinylbenzene resins, (CAT-PS-DVB), with vanadyl acetylacetonate $[VO(AcAc)_2]$ were studied. Vanadyl ion removal from solution at equilibrium was 0.104 mmol V/g of resin and 0.075 mmol V/g resin for the 2% and 20% CAT-PS-DVB resins, respectively. It was found that the 20% cross-linked modified resin was limited in the vanadyl ion ligand-exchange reaction by diffusion into the resin, while this was not the case for the 2% cross-linked modified resin. The effect of the base, triethylamine, dramatically increased the amount of vanadyl ion removed from solution, via ligand-exchange, and was thought to occur by deprotonation of the catechol ligand. The bidentate ligand, bipyridine, had no effect on the removal of vanadyl ion in the ligand-exchange reaction and thus apparently does not form a 1:1 complex with the vanadium catecholate bonded complex. The structures of the vanadium catecholates on the resin were tentatively established by infrared and electron paramagnetic resonance (EPR) spectroscopy to include two vanadium (4+) complexes–a vanadyl bis(catecholate) complex, $[\bigcirc-VO(CAT)_2]^{2-}$, and a distorted tris(catecholate) complex of octahedral geometry, $[\bigcirc-V(CAT)_3]^{2-}$. Scanning electron microscopy (SEM) and energy dispersive analysis (EDX) studies were also performed on the 2% and 20% cross-linked vanadium-containing CAT-PS-DVB resins to clearly show a uniform distribution of vanadium throughout both the resins.

Planned Activities for FY88

We plan to publish a complimentary study on polymer-pendant nickel catecholates.

STUDIES ON THE BONDING OF POLYNUCLEAR HETEROAROMATIC NITROGEN COMPOUNDS TO PENTAMETHYLCYCLOPENTADIENYL-RHODIUM DICATION: NITROGEN VERSUS π-COMPLEXATION

R.H. Fish and H-S. Kim

In recent studies on the regioselective hydrogenation of polynuclear heteroaromatic nitrogen compounds with mononuclear rhodium and ruthenium homogeneous catalysts , it was evident that the substrate nitrogen compound was bound to the catalyst metal center prior to hydrogen transfer. This bonding of the nitrogen heterocyclic compound to the metal center was pivotal for the selective hydrogenation of the nitrogen-containing ring. Therefore, in order to determine more unequivocally the nature of this substrate bonding, i.e., nitrogen (N) versus π-bonding, we have initiated studies on the reactions of several representative polynuclear heteroaromatic nitrogen compounds with pentamethylcyclopentadienylrhodium dication, $[Cp^*Rh^{2+}]$.

The previous limited studies with Cp^*Rh^{2+}. and nitrogen compounds showed π bonding with indole (benzene ring) and, to our knowledge, no other complexes with polynuclear heteroaromatic nitrogen ligands and Cp^*Rh^{2+} have been reported. Thus, we report preliminary findings that dramatically show that the structure of the nitrogen ligand and availability of nonbonding electrons on the nitrogen atom determines N versus π-bonding to Cp^*Rh^{2+}.

Accomplishments During FY87

The general synthetic reaction procedure which we followed is shown in Eq 1:

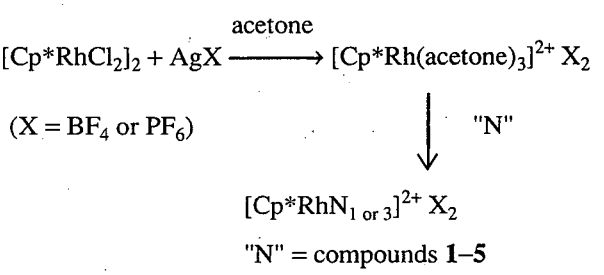

The reactions of quinoline, **1**; 1,2,3,4-tetrahydroquinoline, **2**; 2-methylquinoline, **3**; N-methylindole, **4**; and N-methylpyrrole, **5**, with pentamethylcyclopentadienylrhodium dication $[Cp^*Rh(Acetone)_3^{2+}X_2$, PF_6 or $BF_4]$ were studied to ascertain nitrogen (N) versus π-bonding. Ligands **2**, **3**, **4** and **5** preferred η^6 coordination, while **1** was found to form a tris nitrogen bonded complex.[22]

Planned Activities for FY88

We are presently further evaluating Cp^*Rh^{2+} as a hydrogenation catalyst for polynuclear heteroaromatic nitrogen compounds; obtaining single crystal X-ray analyses for all rhodium complexes; studying the reactions of the rhodium complexes with hydrogen gas and hydride ion; and also studying the bonding of ligands **1-5** with cyclopenadienylruthenium cation.

REFERENCES

1. Ullrich, V. (1972), *Angew. Chem. Int. Ed. 11,* 701, and references therein.
2. (1974) "Molecular Mechanism of Oxygen Activation" O. Hayaishi, Ed., Academic Press, New York N.Y.
3. Guengerich, F.P., MacDonald, T.L. (1984), *Acc. Chem. Res. 17,* 9.
4. Groves, J.T., Nemo, T.E. and Myers, R.S. (1979), *J. Am. Chem. Soc. 101,* 1032.
5. Chang, C.K. and Ebina, F.J. (1981), *Chem. Soc. Chem. Commun.* p. 778.
6. Hill, C.L. and Schardt, B.C. (1980), *J. Am. Chem. Soc. 102,* 6375.
7. Fish, R.H., Kimmel, E.C. and Casida, J.E. (1976), *Advances in Chemistry Series 157,* Organotin Compounds New Chemistry and Applications, J.J. Zuckerman Ed., p. 197.
8. Fish, R.H., Kimmel, E.C. and Casida, J.E. (1975), *J. Organometal. Chem. 93,* C1.
9. Fish, R.H., Kimmel, E.C. and Casida, J.E. (1976), *J. Organometal. Chem. 118,* 41.
10. Fish, R.H., Casida, J.E. and Kimmel, E.C. (1977), *Tetrahedron Lett.,* p. 3515.
11. Fish, R.H., Casida, J.E. and Kimmel, E.C. (1978), *Am. Chem. Soc. Sym., Series No. 82, Organometals and Organometalloids: Occurrence and Fate in the Environment,* Brinckman, F.E. and Bellama, J.M. Eds., p. 82.
12. Kimmel, E.C., Fish, R.H. and Casida, J.E. (1977), *J. Agric. Food Chem. 25,* 1.
13. Kimmel, E.C., Casida, J.E. and Fish, R.H. (1980), *J. Agric. Food Chem. 28,* 117.
14. White, R.E., Miller, J.P., Favreau, L.V. and Bhattacharayya, A. (1980), *J. Am. Chem. Soc. 108,* 6024, and references therein.
15. Momenteau, M. (1986), *Pure and Appl. Chem. 58,* 1493.
16. Momenteau, M., Mispelter, J., Looch, B., and Bisagni, E. (1983), *J. Chem. Soc. Perkin Trans I,* p. 189.
17. Momenteau, M., Mispelter, J., Looch, B., and Lhoste, J.-M. (1985), *J. Chem. Soc. Perkin Trans I,* p. 61.
18. Momenteau, M., Mispelter, J., Looch, B., and Lhoste, J.-M. (1985), *J. Chem. Soc. Perkin Trans I,* p. 221.
19. Bortolini, O., Momenteau, M., and Meunier, B. (1984), *Tetrahedron Lett. 25,* 5773.
20. Mansuy, D., Bartoli, J-F., and Momenteau, M. (1982), *Tetrahedron Lett. 23,* 2781.
21. Fish, R.H., Thormodsen, A.D., Belser, R.B., Jr., Friedman, G., and Reynolds, J.G. (1987), *Reactive Polymers 6,* 255.
22. Fish, R.H. and Kim, H-S. (1987), *Organometallics,* submitted.

Ammonia Removal from Oil Shale Process Waters Using Tubular, Microporous Polytetrafluoroethene Membranes*

R.H. Sakaji, C.G. Daughton, R.E. Selleck, and J.F. Thomas

Ammoniac industrial and domestic wastewaters contain both dissolved ammonia gas (NH_3, a base) and nonvolatile, protonated ammonium ion (NH_4^+, the conjugate acid). The relative concentrations of these two species depends on the pH (pK_a = 9.3 for NH_4^+ at 30°C). The concentration of ammoniac-nitrogen reported for a wastewater does not distinguish between the two forms, and it can range over orders of magnitude: domestic sewage (typically 10 to 50 mg/L),[1] oil refinery wastewaters (as high as 7,000 mg/L),[2] and oil shale process waters (1,000 to 31,000 mg/L).[3]

Ammonia removal from refinery wastewaters typically depends on a packed-bed process, such as energy-intensive steam-stripping. Studies by the American Petroleum Institute have shown that steam stripping is not always effective.[4] Since alternative technologies would be desirable, this project has investigated gas-permeable membrane separation, specifically nonosmotic dissolved-gas dialysis (NOGD), as an alternative to conventional steam stripping.[5] Using NOGD, ammonia diffuses from the wastewater (a region of high concentration) to a dialysate fluid (a region of low concentration) without the concomitant osmosis of liquid water. The semi-permeable separation device comprises tubular polytetrafluoroethene (PTFE) membranes, which combine hydrophobic and microporous properties to allow gases to volatilize from a liquid and diffuse through the gas-filled membrane pores while preventing the passage of liquid water. The wastewater is thereby not diluted by osmosis, and highly concentrated dialysates can be produced. The transport of ammonia is driven by a concentration gradient maintained across the membrane by absorption of the ammonia-gas permeate into a dilute, nonvolatile acid solution, where it is protonated to form ammonium ion. This effectively reduces the ammonia concentration at the outer membrane wall to zero. NOGD would not only be less energy intensive and more selective, it would also succeed in combining stripping and resource recovery into a single unit process; this simplifies design and encourages recovery of a potentially valuable resource (ammonia for fertilizer).

*This work was supported by the Assistant Secretary for Fossil Energy, Office of Oil, Gas, and Shale Technology of the U.S. Department of Energy under Contract No. DE-AC03-76SF00098, through the Bartlesville Project Office, Bartlesville, OK.

ACCOMPLISHMENTS DURING FY 1987

The subject of the work summarized here is a numeric model for the mass transfer of ammonia, with the objective of understanding how ammonia is transported through the PTFE membranes. A detailed numeric model was built from the equation of continuity; effects such as dispersion and diffusion were modeled as separate phenomena. The NOGD process was modeled assuming the wastewater to be an incompressible fluid that is pumped through a tubular membrane with steady laminar flow in a direction, z, parallel to the membrane wall. The velocity profile is fully established and is parabolic. Ammonia is transported only by diffusion in the radial direction and by convection in the z-direction (diffusion in the z-direction is negligible in comparison). The model further assumes that there is no chemical reaction that consumes or produces ammonia while the wastewater is in the PTFE membrane. The equations and method of solution for the set of equations are identical to the "extended Graetz" problem,[6] which can be solved by using the separation-of-variables technique. The accuracy of the computer program used to solve this system was verified and shown to be accurate to four significant figures.[7]

The model was used to calculate average ammonia concentrations in the PTFE reactor effluent, and these were compared with experimental results. A disadvantage in this approach is that changes in the average ammonia concentration θ (the ratio of effluent concentration to influent concentration) over a range of dimensionless residence times γ does not follow a simple proportionality. It was therefore necessary to transform and normalize the data so that changes in θ with respect to γ did not affect the comparison of experimental and predicted data. This was accomplished by determining mass-transfer coefficients, k_{expt} and k_{calc}, from the experimental and predicted average concentrations, respectively.[7]

The numeric model was tested using the experimental results from an isothermal, countercurrent NOGD reactor comprising three concentric tubes: an inner, PTFE tubular membrane, a middle glass tube containing the acid dialysate (sulfuric acid, 1.0 N, was selected as the dialysate acid because it is nonvolatile), and an outer glass tube that served as a

temperature-controlled jacket. The tubular PTFE membranes were manufactured by W.L. Gore and Associates, Inc. (Elkton, MD) (i.d. = 1.0 mm; o.d. = 1.8 mm; maximum pore size = 2.0 μm; porosity = 0.50).

The NOGD reactor was used to treat ammonium hydroxide solutions (700-800 mg-N/L), three oil shale process waters (1,130-24,700 mg-N/L), and a sample of domestic sewage. Samples from the ammonium hydroxide experiments were immediately analyzed for total-N by the rapid method of combustion/chemiluminescence (C/CL).[8] These values were equivalent to ammoniac-N since ammonia was the only nitrogenous compound present. The wastewaters were analyzed for ammonia by the phenate colorimetric method.[3] Composite samples of the effluents were collected after the NOGD reactor reached steady-state operation (more than 100 reactor volumes). Since dissolved ammonia gas rather than ammonium ion was the species of interest, ammonia concentrations were calculated from the sample pH using the pK_a of ammonium ion.

The relationship between the experimental results and predicted values were demonstrated by plotting the experimental versus predicted fraction of ammonia remaining. A perfect correlation would yield a line with a slope of unity and a zero intercept (broken line, Fig. 1). Since the ideal line was within the 95% confidence limits of the regression line for the ammonium hydroxide solution, the difference between the experimental and predicted results was probably not significant. The agreement between predicted values and experimental results indicated that the proposed mechanisms of ammonia transport in the numeric model (i.e., radial diffusion, tortuous gas-phase diffusion through the membrane, and longitudinal convection in laminar flow) accounted for the major transport mechanisms during treatment of an aqueous ammonium hydroxide solution.

Data obtained from the oil shale retort water experiments correlated with predicted values (indicated by regression analysis of the experimental θ against the predicted θ) (Fig. 2). The data deviated significantly (as shown by analysis of variance at 99% confidence level), however, from the ideal correlation (broken line, Fig. 2). The regression lines all lie above the ideal case, an indication that performance was poorer than predicted by the model. The increased resistance to mass transfer possibly resulted from pH-dependent reactions (e.g., production or consumption of ammonia) or physicochemical interactions at the gas-liquid interface (e.g., surfactants, such as fatty acids, which are endogenous to retort waters). Neither of these factors was included in the numeric model.

The ammonia removals from Oxy-6, Paraho, and Geokinetics oil shale process waters (56%, 64%,

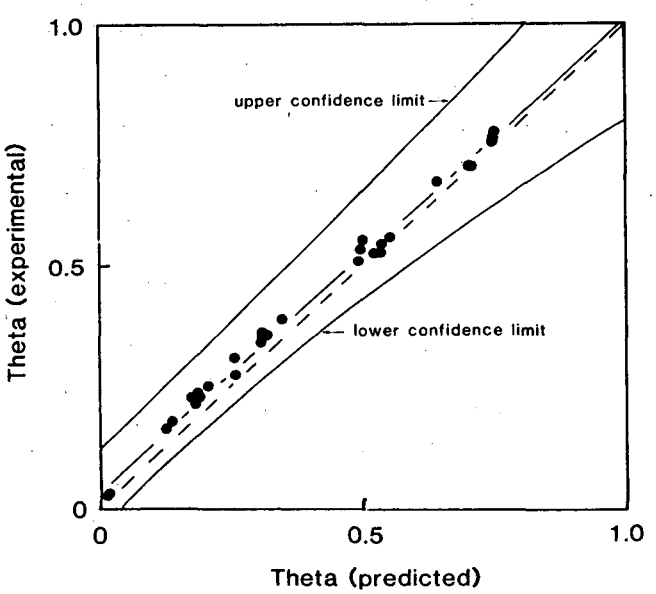

Figure 1. Regression analysis of the experimental fraction remaining (θ) versus the predicted fraction remaining after NOGD treatment of an ammonium hydroxide solution; solid line (least-squares fit), dashed line (ideal fit) with 95% upper and lower confidence limits for the regression line. (XBL 8611-4628)

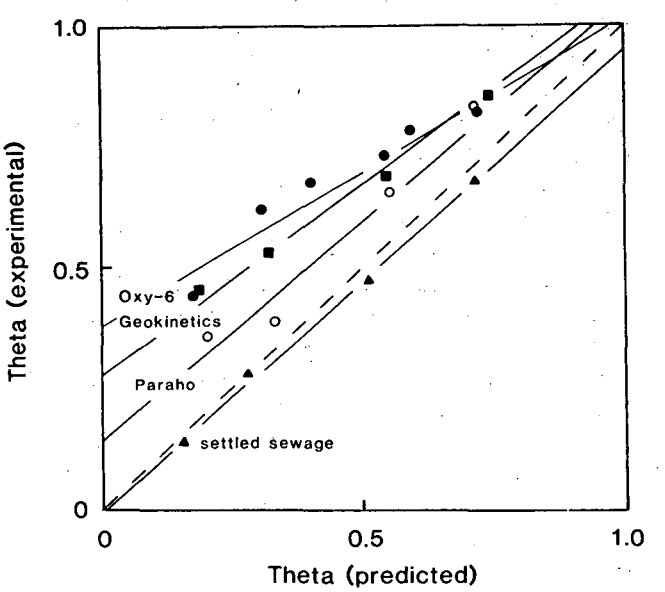

Figure 2. Regression analysis (solid lines) of the experimental fraction remaining (θ) versus the predicted fraction remaining after NOGD treatment of wastewaters: Oxy-6 (solid circles), Geokinetics (solid squares), and Paraho (open circles) oil shale retort waters; domestic wastewater (solid triangles); dashed line (ideal fit). (XBL 8611-4629)

and 55%, respectively) were obtained at hydraulic residence times of 0.92, 0.83, and 0.87 minutes, respectively. These percentage removals are comparable with those of some pilot- and bench-scale steam strippers.[9]

The close correlation between the model and the ammonium hydroxide experimental results suggests that NOGD and the hollow-fiber gas membrane[10] process are identical in principle, even though they differ in operation. In both processes, concentration gradients are associated with the resistance to mass transfer, and because gradients exist only in the water and the membrane, the only resistance to mass transfer would be encountered in those two phases. This in turn means that no resistance to mass transfer exists in the acid dialysate. The NOGD process therefore is not dependent on the flow rate of the dialysate. This is unlike steam stripping, whose physical operation is dependent on the gas-to-liquid (steam-to-wastewater) ratio.

One physical criterion used to compare the relative economies of various stripping devices is the ratio of gas-liquid surface area to empty-bed reactor volume. For a hypothetical NOGD reactor containing 18 tubular membranes packed in a 1.5-cm i.d. dialysate tube, this ratio would be 300 m^2/m^3, which compares favorably with 550 to 820 m^2/m^3 reported for polypropylene hollow-fiber gas membranes[10] and 62 to 980 m^2/m^3 reported for packed-bed reactors.[11]

Since the surface-area-to-volume ratios are within an order of magnitude, the relative differences between the mass-transfer rates will be determined by the mass-transfer coefficients. The mass-transfer rate in the hollow-fiber gas membrane process will be roughly two orders of magnitude below steam stripping or one order of magnitude lower than NOGD. Even though the mass-transfer coefficients for a packed-bed stripper under identical conditions[10] are an order of magnitude better than that found for the NOGD reactor, consideration of NOGD as an alternative to steam stripping should include its lower operating temperature and enhanced resource recovery.

PLANNED ACTIVITIES FOR FY 1988

NOGD has potential as an alternative to steam stripping for removal of ammonia from both domestic and oil shale process wastewaters. The results of numeric modeling imply that it may be possible to improve NOGD process performance by eliminating the reliance on diffusive transport through the use of turbulence promoters. This will be addressed in future experiments. Once the process has been improved, the feasibility of treating other ammoniac wastewaters can be investigated, a more detailed comparison with steam stripping can be made, and a larger-scale reactor can be constructed and tested.

REFERENCES

1. Metcalf and Eddy, Inc. (1979) *Wastewater Engineering,* second edition, revised by G. Tchobanoglous, McGraw-Hill Book, NY.
2. American Petroleum Institute (1969), "Manual on Disposal of Refinery Wastes, Volume on Liquid Wastes," first edition, American Petroleum Institute, Washington, D.C.
3. Daughton, C.G., Sakaji, R.H., and Langlois, G.W. (1986), "Oil Shale Retort Water Ammonia Determination by Titrimetry, Phenate Colorimetry, Enzymatic Analysis, and Chromatographic Fractionation/Chemiluminescence," *Anal. Chem. 58,* 1556.
4. American Petroleum Institute (1975), "Sour Water Stripping Project Committee on Refinery Environmental Control," American Petroleum Institute, Refining Department, Washington, D.C., API Publication 946.
5. Sakaji, R.H., Thomas, J.F., and Daughton, C.G. (1985), "Removal of Ammonia from Wastewater Using Tubular Microporous Polytetrafluoroethene Membranes," Environmental Research Program Annual Report FY 1984, LBL-18754, p. 4-56.
6. Bowen, B.D., Levine, S., and Epstein, N. (1976), "Fine Particle Deposition in Laminar Flow through Parallel-Plate and Cylindrical Channels," *J. Colloid Interface Sci. 54,* 375.
7. Sakaji, R.H., Daughton, C.G., Selleck, R.E., and Thomas, J.F. (1986), "Ammonia Removal from Oil Shale Process Waters Using Tubular, Microporous Polytetrafluoroethene Membranes," in Nineteenth Oil Shale Symposium Proceedings, J.H. Gary Ed., Colorado School of Mines Press, Golden, Colorado, p. 208.
8. Jones, B.M. and Daughton, C.G. (1985), "Chemiluminescence vs. Kjeldahl Determination of Nitrogen in Oil Shale Retort Waters and Organonitrogen Compounds," *Anal. Chem. 57,* 2320.
9. Sakaji, R.H., Persoff, P., and Daughton, C.G. (1984), "Steam Stripping of Oil Shale Wastewaters," Sanitary Engineering and Environmental Health Research Laboratory, University of California, Berkeley, CA, UCB/SEEHRL 84-3.
10. Qi, Z. and Cussler, E.L. (1985), "Hollow Fiber Gas Membranes," *AIChE J. 31,* 1548.
11. Treybal, R.E. (1980), *Mass-Transfer Operations,* third edition, McGraw-Hill Book, NY.

Kinetics of Gas-Phase Reactions Between Ozone and Selected Nitrogen Heterocycles from Oil Shale Wastes*

E.R. Blatchley III, J.F. Thomas and C.G. Daughton

Removal of dissolved organic carbon, much of it in the form of organonitrogen compounds (ONCs), from oil shale process wastewaters has proved difficult, if not impossible, using conventional (and unconventional) treatment methods.[1-3] Since many of these ONCs are volatile, atmospheric emissions are likely. Release of ONCs to the atmosphere could be important because (1) they are not specifically regulated since there are currently no significant sources of emission, (2) they have displayed acute toxicity and mutagenic potential, and (3) many are malodorous and exhibit low odor thresholds. Once released to the atmosphere, a compound's atmospheric lifetime and fate will be determined by various physical and chemical processes. Physical processes include condensation of vapors to form aerosols, settling of particles to the earth, washout by dissolution in precipitation, and transport of vapors and particles through the atmosphere. Photochemical reactions are the driving force behind most atmospheric chemistry. They are directly responsible for the decay of some atmospheric pollutants and are essential in the generation of reactive intermediates such as ozone and free radicals. The atmospheric chemistry of most organic pollutants is dominated by free-radical reactions.

ACCOMPLISHMENTS DURING FY 1987

The kinetics of reactions between ozone and certain methyl-substituted nitrogen heterocycles (NHCs) were investigated. Ozone-NHC reaction kinetics were determined to allow comparison with kinetics of other important reactions involving NHCs. These comparisons will allow for determination of the dominant path for chemical degradation in the atmosphere, which will in turn allow for prediction of atmospheric chemical lifetimes. The objective was to determine second-order rate constants for reactions between individual NHCs and ozone. Reactions were assumed to be second order overall, first order in each reactant. Decreases in ozone concentration were assumed to result from reaction with the NHC and from "non-reactive" losses (e.g., collision with reactor walls). Under these assumptions, the time-dependent ozone concentration is described by:

$$d[O_3]/dt = -k_w[O_3] - k[O_3][NHC], \qquad (1)$$

where $[O_3]$ and [NHC] are ozone and NHC concentrations, respectively, k_w is a "wall" rate constant, and k is the second-order rate constant. If $[NHC]/[O_3] >> 1$, then [NHC] will remain essentially constant over time, and the reaction can be described using pseudo-first-order kinetics. Under the assumption that [NHC] is a constant, equation (1) can be solved to give the following analytical solution:

$$\ln([O_3]_0/[O_3]_t) = k't \qquad (2)$$

where k′ is a pseudo-first-order rate constant = k_w + k[NHC]. Equation (2) was used as the basis for experimental design.

An apparatus was designed to allow introduction of known quantities of ozone, air, and individual, pure, vapor-phase NHCs to an evacuated reaction chamber. After introduction of reactants, the reaction chamber was pressurized to 760 mm Hg with ultra-zero air, magnetically stirred, and maintained at room temperature; these conditions approximated those of the troposphere on a mild day. The NHC concentration was monitored using a chemiluminescent nitrogen-analyzer and capillary gas chromatography with flame ionization detection, and ozone concentration was monitored with absorbance scans from 350 to 200 nm using a UV-vis scanning spectrophotometer. Chromatographic analysis of the reactor contents, before and after ozone reactions, confirmed that NHC concentrations remained essentially constant.

From equation (2), a plot of $\ln([O_3]_0/[O_3]_t)$ vs. t yields a line through the origin with slope = k′. For each NHC examined, several values of [NHC] were evaluated, and k′ was determined for each. Each NHC seemed to obey pseudo-first-order kinetics, although some deviations were observed. A plot of k′ vs. [NHC] is linear with slope of k and intercept of k_w. Second-order rate constants were determined for each of the NHCs (Table 1). The compounds selected represent a majority of expected gaseous organonitrogen emissions from oil shale development.

Ozone is a strong oxidizing agent. Therefore, the availability of a compound's electrons for reaction will determine its reactivity with ozone. The aromatic character and electronegativity of the

*This work was supported by the Assistant Secretary for Fossil Energy, Office of Oil, Gas, and Shale Technology of the U.S. Department of Energy under Contract No. DE-AC03-76SF00098, through the Bartlesville Project Office, Bartlesville, OK.

Table 1. Second-order rate constants and atmospheric lifetimes[a] for reaction of NHCs with O_3.

Compound	k (10^{-19} cm^3/molec-min)	lifetime[b] (years)
pyridine	1.1	14
2-methylpyridine	2.7	5.8
2,6-dimethylpyridine	3.1	5.0
4-methylpyridine	5.9	2.6
3-methylpyridine	6.0	2.6
2,5-dimethylpyridine	23	0.7
benzene[c]	6.0	2.6
pyrrole[d]	9600	14 (hours)

[a]Values of atmospheric lifetime are based on an assumed ozone concentration of 0.05 ppm.
[b]Atmospheric lifetime is defined as the time required to reduce the concentration of a reactant by a factor of "e", where ln(e) = 1.
[c]Data from reference 4.
[d]Data from reference 5.

aromatic nitrogen atom make the NHCs studied (all were six-membered rings) pi-electron deficient (relative to benzene), and hence relatively non-reactive towards ozone. The kinetics determined in these experiments suggest that reactions involving ozone will not be important in reducing the atmospheric lifetime or in determining the fate of these NHCs. Previous experiments have suggested that direct photochemical reactions are also too slow to be of any significance.[6]

We suspect that the most important mode of chemical transformation for these NHCs in the atmosphere will be free-radical reactions; those involving the hydroxyl free radical are likely to dominate. Since free radical reactions also rely on the availability of electrons for reaction, it seems likely that these radical-mediated reactions will also be slow. If so, then the fate of these NHCs in the atmosphere may be determined by physical rather than chemical processes. Compounds with long chemical lifetimes in the atmosphere are significant in that they can be used as tracers of pollution. Since NHCs have such low natural atmospheric abundance, increases in concentration of NHCs downwind from synfuel development sites could possibly be used as indicators of atmospheric pollution.

PLANNED ACTIVITIES FOR FY 1988

Experiments are planned to determine rate coefficients for reactions between NHCs and hydroxyl radical ($OH^{\bullet}$). Previous studies have found hydroxyl radical reactions to dominate the atmospheric chemistry of many organic compounds. The reactions involving NHCs and hydroxyl radical are still likely to be slow relative to the atmospheric reactions of many organic compounds because of the NHC's low pi-electron density.

REFERENCES

1. Healy, J.B., Jr., Jones, B.M., Langlois, G.W., Thomas, J.F., and Daughton, C.G. (1984), "Biotreatment of Oil Shale Wastewaters Using Batch Cultures and Fixed-Film Reactors," Environmental Research Program Annual Report FY 1983, LBL-17073, p. 4-35.
2. Jones, B.M., Langlois, G.W., Sakaji, R.H., Thomas, J.F., and Daughton, C.G. (1983), "Oil Shale Wastewater Treatment: Effect of Ozonation and UV Irradiation on Biorefractory Organic Solutes," Environmental Research Program Annual Report FY 1982, LBL-15298, p. 4-44.
3. Daughton, C.G., Jones, B.M. and Sakaji, R.H. (1985), "Organic Nitrogen Determination in Oil Shale Retort Waters," *Anal. Chem. 57*, 2326.
4. Finlayson-Pitts, B.J. and Pitts, J.N., Jr. (1986), *Atmospheric Chemistry*, John Wiley & Sons, NY, p. 633.
5. Atkinson, R., Aschmann, S.M., Winer, A.M., and Carter, W.P.L. (1985), "Rate Constants for the Gas-Phase Reactions of NO_3 Radicals with Furan, Thiophene, and Pyrrole at 295 ± 1 K and Atmospheric Pressure," *Environ. Sci. Technol. 19*, 87.
6. Blatchley III, E.R., Thomas, J.F., and Daughton, C.G. (1986), "Sunlight Reactions of Volatile Organonitrogen Emissions from Oil Shale Wastewaters," Environmental Research Program Annual Report FY 1985, LBL-20204, p. 4-52.

Separations by Reversible Chemical Association*

C.J. King, A.S. Kertes, D. Arenson, J. Tamada, W. Rixey, A. Garcia, L. Poole, and M. Ng

Carboxylic acids, alcohols, glycols and related polar-organic substances are potentially attractive for manufacture from biomass by fermentation. These products must be recovered from highly dilute and complex solutions. Separations based upon reversible chemical association (complexation), using reactive extractants or sorbents, offer better selectivity and lower energy consumption than occur for approaches involving evaporation or distillation of water.

This research involves measurement, modeling and interpretation of phase equilibria and transport for these separations. Further goals are to define rational criteria for selecting complexation reagents, to develop suitable methods for regeneration, and to define the most likely applications. These goals require both chemical and process insight.[1,2]

A related sub-project has explored the use of non-wetting, non-functional macroreticular polymeric adsorbents for selective recovery of these same solutes from dilute aqueous solutions.

The initial phase of the project included literature surveys of the extraction chemistry of carboxylic acids and alcohols.[3,4]

ACCOMPLISHMENTS DURING FY 1987

Extraction of Carboxylic Acids

Equilibria have been measured for extraction of succinic, acetic, lactic and malonic acids by mixed trioctyl and tridecyl amines, with either methyl isobutyl ketone, chloroform or n-heptane as diluent. The results have been rationalized through chemical modeling[5] and show (a) favorable extraction equilibria, (b) overloading of the amine with acid, (c) a molar ratio of water to extracted acid that is different for different carboxylic acids, and (d) substantial effects of temperature and the nature of the diluent.

Three methods for regenerating low-volatility acids from amine extractants have been investigated experimentally – changing temperature to create a more favorable equilibrium for back-extraction into water, changing the composition of the diluent between forward- and back-extraction for the same purpose, and back-extraction into aqueous ammonia, followed by concentration of the aqueous solution and thermal decomposition of the ammonium carboxylate. Studies of regeneration by the latter method have shown that amides are formed irreversibly when ammonium carboxylates are heated. We have now improved this method by replacing ammonia with trimethylamine, which cannot form amides.

Extraction of Alcohols

We earlier found that phenols are effective extractants for alcohols. Equilibria have been measured for extraction of ethanol from aqueous solutions by m-cresol and other phenolic extractants with various diluents, and are being interpreted through chemical modeling.[6] The results so far suggest a 1:1 complex between ethanol and the phenolic extractant. The experiments, modeling and interpretation are complicated by the large number of competing equilibria, and the fact that the various hydrogen bonds formed among alcohols, phenols, water and many of the diluents are of comparable strengths.

The addition of alkyl or halogen substituents to a phenolic extractant has a relatively small effect upon the molar equilibrium distribution coefficient.

Functionalized Polymeric Sorbents

Solid sorbents are potentially non-contaminating. A number of basic polymeric sorbents were tested for recovery of acetic acid from aqueous solution. Properties measured included equilibrium sorption capacity, water uptake, and regenerability either by solvent leaching or by heating and vaporization. The sorbents contained primary, secondary and tertiary amine, pyridyl, amide, N-oxide, and imidazole functional groups.

Equilibrium sorption capacities have been successfully interpreted through a chemical-exchange model, relating the capacity to the density of accessible functional groups and an affinity constant related to the basic strength, as represented by the Gutmann Donor Number. Water is taken up by pore filling and swelling. Swelling has been related to osmotic pressure.

Exploratory studies have been made of regeneration of acetic acid from amine, pyridyl and imidazole resins. Pyridyl sorbents can be regenerated by common solvents (e.g., methanol) at ambient tem-

*This work was supported by the Assistant Secretary for Conservation and Renewable Energy, Office of Energy Systems Research, Energy Conversion and Utilization Technologies (ECUT) Division of the U. S. Department of Energy under Contract No. DE-AC03-76SF00098.

perature, but the other basic groups are much less amenable to regeneration by solvent leaching.

Dowex WGR, a high-capacity amine sorbent, can be regenerated by aqueous ammonia solution, which can be followed by thermal decomposition of the ammonium carboxylate to enable recovery of the carboxylic acid and recycle of ammonia. Again, it may be desirable to use a low-molecular-weight tertiary amine rather than ammonia, so as to avoid amide formation.

Thermal degradation hampers regeneration of polymeric sorbents by heat and vaporization. However, Dowex MWA-1, a high-capacity tertiary amine sorbent, can be regenerated by heating to 100°C for several hours. Celanese Aurorez, a polybenzimidazole, is stable to very high temperatures but undergoes a surface-sealing phenomenon if heated in the presence of imbibed water. These results suggest several avenues for improved regeneration.

Non-Wetting Adsorbents

Because of low water uptake, non-wetting macroreticular styrene-divinylbenzene adsorbents are potentially attractive for recovery of polar organics from dilute aqueous solution. Since the rate-limiting step is Knudsen diffusion within air-filled pores, these adsorbents can also fractionate among solutes with different volatilities.[7]

Fixed-bed studies with non-wet adsorbents showed that it is important to purge interstitial air with water before introducing the feed to be fractionated. The degree of separation among components was interpreted quantitatively by allowance for axial dispersion and rates of Knudsen diffusion within the pores.[8]

PLANNED ACTIVITIES FOR FY 1988

Regeneration of Extractants and Adsorbents

Improved regeneration is the greatest need for economical recovery of carboxylic acids by complexing extractants or sorbents. The thermodynamics of extraction of carboxylic acids by tertiary amines will be examined to seek ways of obtaining large effects of temperature and/or diluent change upon extraction equilibria, thereby facilitating regeneration by back-extraction following changes in temperature and/or diluent.

Phase equilibria will be determined for regeneration of amine extractants and sorbents by back-extraction with aqueous trimethylamine, and thermal decomposition tendencies of the resulting trimethylammonium carboxylates will be measured. Two additional regeneration methods to be explored are precipitation of low-solubility carboxylic acids (e.g., fumaric) and displacement of extracted or sorbed carboxylic acid by a stronger acid, which is more readily regenerated. Improved thermal regeneration of poly(benzimidazoles) will be sought through methods which avoid or reduce surface sealing.

Extractants and Sorbents

Systematic development of improved sorbents will be pursued by complementing chemical insight with improved understanding of the effects of the morphology of the solid on capacity, water uptake and regenerability.

Extraction equilibrium data will be obtained for additional carboxylic acids, so as to enable generalizations about affinity constants and tendencies for overloading of amine extractants, co-extraction of water, and regeneration by various means. Spectroscopic measurements will be made where appropriate and useful for confirming association stoichiometry. Extraction equilibria for recovery of glycols with phenolic extractants will be measured and interpreted, and stronger extractants for alcohols and glycols will be sought. Sorbents or polymeric extractants with pendant phenol groups (e.g., polyvinylphenol) will be investigated for recovery of alcohols and glycols.

REFERENCES

1. King, C.J. (1987), in *Handbook of Separation Process Technology,* Chap. 15, R.W. Rousseau, ed., John Wiley & Sons, New York.
2. King, C.J. (1988), *Proc. Intl. Solvent Extraction Conf. (ISEC'88),* Moscow, USSR.
3. Kertes, A.S. and King, C.J. (1986), *Biotechnol. Bioeng. 28,* 269.
4. Kertes, A.S. and King, C.J. (1987), *Chem. Rev. 87,* 687.
5. Tamada, J.A., Kertes, A.S. and King, C.J. (1988), *Proc. Intl. Solvent Extraction Conf. (ISEC'88),* Moscow, USSR.
6. Kertes, A.S., Arenson, D.R., and King, C.J. (1988), *Proc. Intl. Solvent Extraction Conf. (ISEC'88),* Moscow, USSR.
7. Rixey, W.G. and King, C.J. (1987), in *Fundamentals of Adsorption – II,* A.I. Liapis, ed., Engineering Foundation, New York.
8. Rixey, W.G. (1987), Ph. D. Dissertation, Dept. of Chemical Engineering, Univ. of California, Berkeley, CA.

Differential Photothermal Deflection Spectroscopy*

R.E. Russo, J.D. Spear, and R.J. Silva†

Photothermal deflection spectroscopy (PDS) has been recognized for its ability to measure ultrasensitive radiative absorption in transparent media. Unlike conventional beam-transmittance spectrophotometry, PDS directly measures the absorbed radiation by monitoring temperature gradients produced within the medium. However, for liquid-phase analysis, absorption by the solvent (background) limits the sensitivity of analysis. We developed a dual-beam, differential PDS system using a split probe-beam arrangement with a single position sensor and detection electronics to correct for background absorption.

ACCOMPLISHMENTS DURING FY 1987

The optical arrangement of this PDS system is shown in Fig. 1. An argon-ion pumped dye-laser, modulated at 80 Hz, provided the excitation radiation. A linearly polarized helium-neon laser served as the probe-beam source. The excitation and probe lasers strike opposite sides of a dielectric beam splitter at nearly equal angles of incidence. The beam splitter produced two sets of excitation and probe beams which overlap in a sample cuvette (S) and a reference cuvette (R). Lenses (L_1 and L_2) are placed before the beam splitter and focus the excitation and probe beams in the centers of the cuvettes. Within each cuvette, both the excitation and probe beams are horizontal, intersecting each other at an angle of ~0.5°. The axis of the probe beam is aligned slightly above that of the excitation beam. The position detector is a single-axis, solid-state, photodetector with an attached interference spike filter that passes only the light from the HeNe probe beam. The position detector signal is conditioned and fed into a lock-in-amplifier.

The conventional PDS approach is to monitor the deflection of both beams with two separate position detectors and additional related electronics. However, this approach is limited because of electronically subtracting uncorrelated signals. Our PDS system avoided this problem by folding the reference probe beam back into the path of the sample probe beam so that only a single position detector was needed (cf. Fig. 1). Two mirrors (M_1 and M_2) and a prism (P) allowed the two probe beams to overlap on the detector. The placement of an additional lens

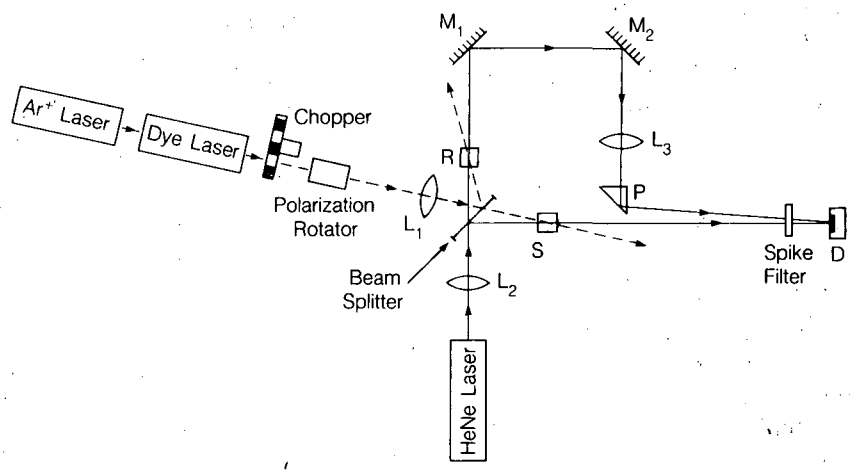

Figure 1. Optical arrangement of the dual-beam, differential photothermal deflection spectroscopy (PDS) system. (XBL 8711-9102)

*This work was performed under the Lawrence Livermore National Laboratory Contract No. W-7405-ENG-48 for the U.S. Department of Energy.

† Nuclear Chemistry Division, Lawrence Livermore National Laboratory.

(L_3) in the reference beam path was necessary to make its deflection subtractive, rather than additive, to that of the sample probe beam.

If the relative intensities of the reference and sample probe beams at the detector are equal, then the position sensor measures their average deflection. Because the reflectance of the beam splitter depends on the polarization of incident light, these relative intensities were balanced by rotating the cylindrical probe laser head about its longitudinal axis until the beam's polarization was near 45° from vertical. Similarly, an adjustable polarization rotator was placed before the beam splitter to balance the relative intensities of the excitation beams in the reference and sample cuvettes, so that comparable deflection amplitudes would result when the two cuvettes contained similar solutions.

Background correction and sensitivity were demonstrated by using a dilute solution (10^{-5} M) of Nd^{3+} in 10^{-2} M HCl. Neodymium has a narrow absorption line at 575 nm with a molar absorptivity of only 6.9 L $mole^{-1}cm^{-1}$. The reference cell contained only the solvent. The spectra in Fig. 2a were obtained by alternately removing the reference and the sample solutions. The absorption of 10^{-5} M Nd^{3+} in HCl (I) provided a positive deflection signal, while the absorption of the reference HCl (II) provided a negative deflection signal. The background absorption of the solvent obscured the absorption spectrum of the neodymium at this concentration. However, when the system was operated with both solutions in place, the correct absorption spectrum for 10^{-5} M Nd^{3+} was measured (Fig. 2b). Thus, real-time, differential background correction provided an increase in PDS sensitivity.

PLANNED ACTIVITIES FOR FY 1988

A differential dual-beam thermal lensing spectroscopy (TLS) system will be developed and compared to the PDS system. In addition, the possibility of performing TLS and PDS at the end of optical-fibers will be explored.

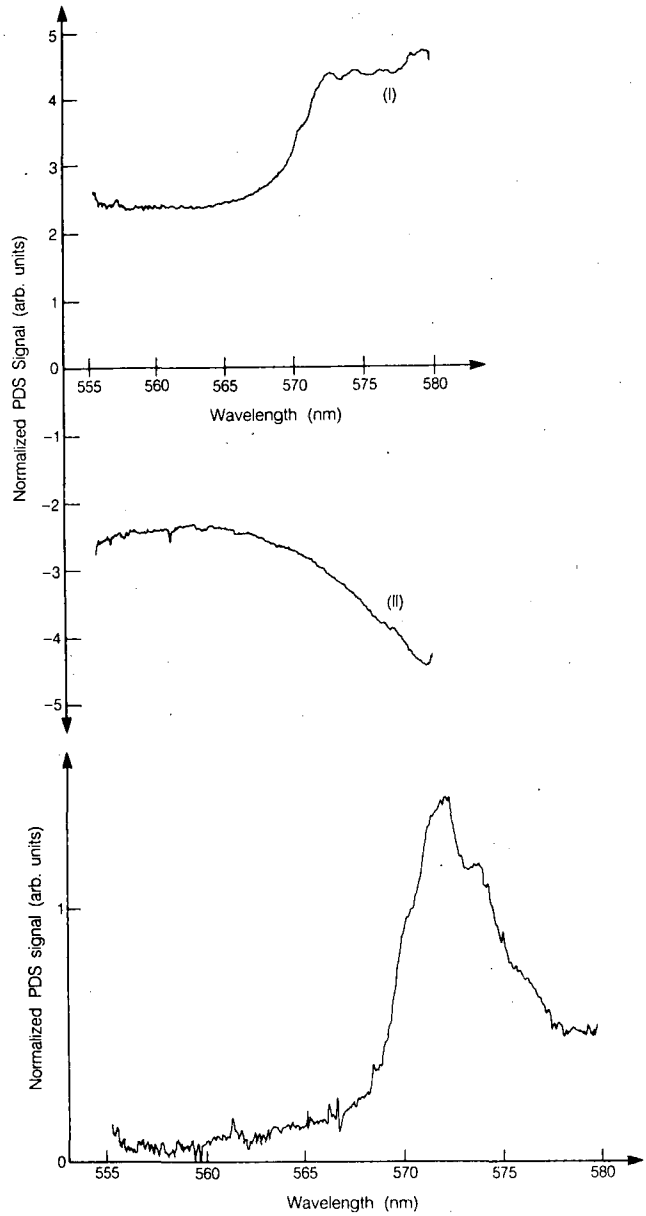

Figure 2. PDS signal for a) 10^{-5} M Nd^{3+} (I) and 10^{-2} M HCl (II) without background correction, and b) with background correction. (XBL 8711-9100A)

LAWRENCE BERKELEY LABORATORY
TECHNICAL INFORMATION DEPARTMENT
UNIVERSITY OF CALIFORNIA
BERKELEY, CALIFORNIA 94720